Assessment of remotely piloted aircraft data classification of wetland vegetation communities and changes in their pattern with elevation

by

Brandon Giura

A thesis

presented to the University of Waterloo

in fulfillment of the

thesis requirement for the degree of

Master of Science

in

Geography

Waterloo, Ontario, Canada, 2023

© Brandon Giura 2023

Author’s Declaration

I hereby declare that I am the sole author of this thesis. This is a true copy of the thesis, including any required final revisions, as accepted by my examiners.

I understand that my thesis may be made electronically available to the public.

Abstract

Wetlands host a myriad of services both to the environment and society. While the provision of those services are partly dependent on the terrestrial plant communities that both comprise and are adjacent to a wetland, little has been done to map these communities at high spatial resolutions or measure their composition and configuration. Remotely piloted aircraft (RPA) have been used to capture very-high resolution imagery that can aid our understanding of wetland characteristics and function without harming the local environment. However, a gap remains in our understanding of the composition and configuration of vegetation communities in high-elevation wetlands. As a step toward improving our understanding, an RPA was used to collect multi-spectral data (red edge, green, blue, near infrared) and analyzed to determine the ability to identify and map the composition and configuration of wetland vegetation communities at high elevations in Alberta, Canada. These wetlands have been excluded from the Canadian Wetland Classification System mapped areas. In addition to assessing the ability for automated classification of vegetation communities in an object-based image analysis, the relative contribution each spectral band, their combination in different indices (e.g., NDVI), and a generated digital surface model had on classification accuracy was quantified. Results from a random tree classifier obtained an overall accuracy of 91.43%, total producer's accuracy of 86.9% and total user's accuracy of 92.7%. Of 17 inputs (12 image layers and 5 objects features) included in the classifier, the Digital Surface Model had the greatest overall importance (average of 15.9%). While comparison between the classifier and testing samples derived through manual segmentation selection yielded high accuracies, comparison of the automated classification against ground survey plots were substantially less accurate (total overall accuracy 54.5%). Analysis of the composition and configuration of the classified RPA data identified five non-correlated landscape metrics that showed statistically significant differences when wetlands were compared across a gradient in elevation. These results demonstrate that elevation can affect the pattern of wetland vegetation and that further research should be done to determine if and how these pattern changes may affect specific wetland functions. In addition to situating the aforementioned results among the broader literature, the potential for improved vegetation mapping with

remotely piloted aircraft is discussed along with the need for a standard set of reporting variables for RPA data collection to facilitate comparative analyses.

Acknowledgements

I'd first like to thank Alberta Innovates and the National Sciences and Engineering Research Council (NSERC) of Canada which provided the funding for this research.

Dr. Derek Robinson, there aren't enough "Thank Yous" I can provide for everything you have done throughout this journey. From the opportunity to join the research team, the constant mentorship and encouragement, the laughs and many stops for food after long days in the field flying drones. I'm so grateful I could be part of it.

Further thanks to those who accompanied me out in those farm fields on those hot days to collect data, John and Chris Giura, Kyle Giura and Jacy Boegel. I literally couldn't fly without your eyes, and I haven't forgotten that I still owe you all lunch.

Lastly, I'd like to thank all the colleagues and friends I made along the way. Specifically, within the office, Chelsea, Renan, Dora (Chenxi), Sri and Amerald - ya'll are great! Can't forget about the Bio group, Hadeel, Tim, Harshina and Anjali.

Dedication

I’d like to dedicate this thesis to my parents (John and Chris). The provided support and guidance have been critical in helping me reach my goals and shaping me into the person I am today.

Mom and Dad, your dedication to my growth and emphasis to the significance of higher education, despite neither of you having the opportunity to pursue it instilled the drive and perseverance to accomplish this.

Cheers.

Table of Contents

Author's Declaration ii

Abstract iii

Acknowledgements v

Dedication vi

List of Figures ix

List of Tables x

List of Abbreviations xi

Chapter 1 : Geomatics and Wetland Mapping 1

Chapter 2 : Assessment of remotely piloted aircraft data classification of wetland vegetation communities and changes in their pattern with elevation 5

1.0 Introduction 5

2.0 Methods 7

2.1 Study Area 7

2.2 Data 10

2.2.1 RPA Survey and Data Creation 10

2.2.2 In-situ survey 11

2.3 Object-Based Image Analysis (OBIA) with eCogition 12

2.3.1 Automated Vegetation Community Classification 12

2.3.2 Training Site Selection 13

2.3.3 Random Tree Classifier 15

2.4 Accuracy Assessment 15

3.0 Results 16

3.1 Accuracy Classification against training samples 16

3.2 Image Layer and Object Feature Importance for Random Tree Training 19

3.3 Comparison of Ground Survey and RPA Classification 22

3.4 Composition and Configuration 24

4.0 Discussion 30

4.1 Accuracy acquisition challenges 32

4.2 Future vegetation mapping with remotely piloted aircraft 36

5.0 Conclusions 38

Chapter 3 : Wetlands and wetland mapping in Canada 40

References 45

Appendix A *Maps (Increasing in Elevation)* 60

List of Figures

Figure 1: Study area showcasing 18 study site wetlands flown via RPAS with the natural subregions with the area of interest (Numbers correspond to the Site No. provided in Table 2) 9

Figure 2: Composition and configuration of both landscape and class metrics that returned statistical significance p lotted against elevation. A) Patch Cohesion Index (PCI) – Landscape Level (p = 0.01), B) Interspersion and Juxtaposition Index (IJI)- Landscape Level (p = 0.04), C) Coefficient of Variation of Patch Area (CVPA) – Class Level (Mixed Vegetation) (p = 0.04), D) Coefficient of Variation of Euclidean NN Distance (CV-ENN) – Class Level (Mixed Vegetation) (p = 0.00), E) Number of Disjunct Core Areas (NDCA) – Class Level (Mixed Vegetation) (p = 0.04) 29

Figure 3: Standout misclassifications during comparison: litter classified as Dirt/bare ground (a/b), rock classified as moss (c/d), Litter classified as Mixed Veg (e/f) and water classified as moss (g/h). All images were captured at a scale of 1:25; Cyan blue square represents the field equipment (quadrat) used by the field team. 35

List of Tables

Table 1: Classification of quadrats based on ground sampling of vegetation composition (Iljas, 2022) 12
Table 2: Vegetation and land cover classes for classification 14
Table 3: Surveyed locations sorted by elevation (Includes Site Number, Natural Subregion, Municipality, Elevation and Overall Accuracy) 17
Table 4: Summary of user's and producer's accuracy for all classified wetlands (including average and standard deviation) 19
Table 5: Weighted importance of each layer used to train the RT classifier (Includes average and standard deviation) 21
Table 6: In situ ground survey comparison with removal of classes that did not obtain a minimum sample size of 50 and aggregation of Broadleaf into Mixed Vegetation 23
Table 7: Vegetation classification conducted using remotely piloted aircraft (RPA). NL = Not listed 32
Table 8: Inventory accuracies for peatland mapping in Canada. Observes overall accuracy (OA), producer's accuracy (PA) and user's accuracy (UA). NL = Not Listed 43

List of Abbreviations

ABMI – Alberta Biodiversity Monitoring Institute

ASL – Above Sea Level

CMOS – Complementary Metal Oxide Semiconductor

CV-ENN – Coefficient of Variation of Euclidean Nearest Neighbour Distance

CVPA – Coefficient of Variation of Patch Area

CWCS – Canadian Wetland Classification System

DEM – Digital Elevation Model

DSM – Digital Surface Model

DJI – Da-Jiang Innovations

GCI - Green Chlorophyll Vegetation Index

GCP – Ground Control Points

GNDVI - Green Normalized Difference Vegetation Index

GNSS -Global Navigation Satellite System

GRVI - Green-Red Vegetation Index

IJI – Interspersion and Juxtaposition Index

LiDAR – Light Detection and Ranging

LULC – Land Use and Land Cover

mB – Mean Blue

mG – Mean Green

mGCI – Green Chlorophyll Vegetation Index

mGNDVI - Green Normalized Difference Vegetation Index

mGRVI – Mean Green-Red Vegetation Index

mNDVI - Normalized Difference Vegetation Index

mNDWI – Normalized Difference Water Index

mOSAVI - Optimized Soil Adjusted Vegetation Index

mR – Mean Red

mRECI - Red Edge Chlorophyll Vegetation Index

mSAVI - Soil Adjusted Vegetation Index

NDCA – Number of Disjunct Core Areas

NDRE - Normalized Difference Red Edge Vegetation Index

NDVI – Normalized Difference Vegetation Index

NDWI - Normalized Difference Water Index

NIR – Near Infrared

OA – Overall Accuracy

OBIA – Object Based Image Analysis

OSAVI - Optimized Soil Adjusted Vegetation Index

PA – Producer's Accuracy

PAm – Mean Producer's Accuracy

PAsd – Producer's Accuracy Standard Deviation

PCI – Patch Cohesion Index

RE – Red Edge

RECI - Red Edge Chlorophyll Vegetation Index

RGB – Red, Green, and Blue

RPA – Remotely Piloted Aircraft

RPAS – Remotely Piloted Aircraft Systems

RT – Random Tree

SAVI - Soil Adjusted Vegetation Index

SfM-MVS - Structure-from-Motion Multi-View Stereo

Site No. – Site Number

UA – User’s Accuracy

UAm – Mean User’s Accuracy

UAsd – User’s Accuracy Standard Deviation

UAV – Unmanned Aerial Vehicle

Chapter 1: Geomatics and Wetland Mapping

Geomatics was offered as a field of study in Canada for the first time in 1986 at Laval University (Gagnon and Coleman, 1990). Defined as “a systemic, multidisciplinary, integrated approach to selecting the instruments and the appropriate techniques for collecting, storing, integrating, modeling, analyzing, retrieving at will, transforming, displaying, and distributing spatially georeferenced data from different sources with well-defined accuracy characteristics and continuity in a digital format.” (Gomarasca, 2010, p.137), geomatics has a breadth of applications and remains important to the study and advancement of multiple disciplines. Geomatics have played an important role in urban planning (e.g., utilities and infrastructure), environmental monitoring (e.g., air and water quality), agriculture (e.g., pest control and crop health), disaster management (e.g., effects of flooding and fire) and natural resource management (e.g., erosion and pollution). The widespread integration of the field of geomatics with other domains is partly because of the technologies that comprise and are used within the field of geomatics such as Global Navigation Satellite Systems (GNSS), which provides precise locational information, and remote sensing (e.g., satellites and aerial systems), which provides information about features on the Earth’s surface via sensors like LiDAR (i.e., terrestrial, and airborne) and the data collected through these technologies are often stored, managed, analyzed and visualized within a Geographic Information Systems (GIS; ESRI, 2023).

Among the many domains to which Geomatics, along with remote sensing, has contributed, includes its use in the domain of wetland ecology has made significant contributions. Airborne data (e.g., Satellite and aerial imagery) have been used to identify the boundaries of wetlands (i.e., Fuller et al., 2006) and provide a better understanding of the extent and distribution of wetlands (i.e., Weise et al., 2020). With the ability to capture different spectral bands (i.e., Red, Green, Blue, NIR), different sensors are used to identify land covers (i.e., Tian et al., 2016), vegetation types (i.e., Pande-Chhetri et al., 2017), and delineate wetland water bodies (i.e., Wu and Lane, 2016). Spectral indices such as the Normalized Difference Vegetation Index (NDVI) has been used to understand vegetation health and classify vegetation (i.e., Ju and Bohrer, 2022; Petus et al., 2013). While other indices such as the Normalized Difference Water Index (NDWI; McFeeters, 1996) has been used to identify water features (i.e., Teng et al., 2021). The spatial data acquired from these sensors can be

utilized within Geographic Information Systems (GIS) (i.e., ArcGIS, ESRI,2023; QGIS, QGIS, 2023 Association) to further visualize and analyze data. GIS provide users the ability to create and effectively combine the different data layers to better understand wetlands. The exported maps become an effective visual aid to better inform decision makers in wetland conservation and environmental monitoring.

Perhaps the most influential sensor affecting our understanding of wetland ecosystems is Light Detection and Ranging (LiDAR). The active sensor emits pulses of visible light photons and can capture information about the distribution of their return to the sensor. The short wavelength (e.g., 1064nm; Newport Corporation, 2023) of these sensors can penetrate the vegetation canopy, which enables the acquisition of information about the surface topography and the creation of highly detailed Digital Elevation Models (DEMs). LiDAR has been used to distinguish different classes of wetlands based on their makeup (i.e., peatlands; Anderson et al., 2010), map vegetation types (i.e., Maxa and Bolstad, 2009) and map inundation levels (i.e., Huang et al., 2014). Overall, the ability for LiDAR to capture data not available through other technologies enhances the use of geomatics in wetland mapping and provides crucial information for conservationists and land-use planning.

While the acquisition of remotely sensed data and the management, analysis, and visualization of those data with a GIS has advanced wetland ecology, the relationship of those data to in-situ measurements is essential for scaling field-based measurements to larger spatial extents. The location of in-situ measurements is often done through the use of Global Navigation Satellite System receivers, which are commonly (and incorrectly) referred to as Global Positioning System (GPS) in North America. The advancements of GNSS receivers have played an important role in geomatics and wetland mapping with its ability to ground truth and validate remotely sensed data (i.e., Rebelo et al., 2009). GNSS receivers can identify exact locations on the ground with precision and verify the accuracies of remote sensing data. Ground truthing is crucial because it ensures the accuracy of a wetland's topography and vegetation species (i.e., Hladik and Alber, 2012) providing a more comprehensive understanding of wetland ecosystems. With a GNSS receiver, it is possible to identify sampling locations (e.g., random, or not) for vegetation ground surveys and land-use change detections over time (i.e., Olofsson et al., 2014). Overall, precise, and reliable wetland

mapping cannot be completed without the inclusion of GNSS equipment and enhances the management of wetlands.

In addition to the aforementioned technologies and tools, Geomatics also plays a pivotal role in modelling and using models to understand the importance of the hydrological system in wetlands and how wetland functions interact with hydrology. Using a GIS, surface flow pathways can be modelled (i.e., Wu and Lane, 2017), watershed and wetland catchments can be mapped (i.e., Watershed – Spatial Analyst Tool, ESRI) and areas prone to erosion can be determined (i.e., Hernández-Romero et al., 2022). Also, the inclusion of remotely sensed data provides valuable information on the landcover and topography (e.g., terrestrial and bathymetry) to further enhance the accuracy of hydrological modeling. For example, airborne data (e.g., Optical, multispectral, and hyperspectral) can give information on an wetlands landcover and LiDAR can map the wetlands terrain (i.e., Jeziorska, 2019). When paired together researchers can create a more accurate representation of a wetland's terrain (i.e., Maxa and Bolstad, 2009). Overall, combining different types of data improves hydrological modelling, providing useful information for managing water resources and the conservation of wetlands.

Furthermore, geomatics within wetland mapping contains the ability to integrate data from many different services and activities. With all the different types of data technologies (e.g., remote sensing, GPS, Field measurements) GIS software provides the ability to store geospatial data within a container called a geodatabase. This storing allows the combination of different data types from multiple sources to be analyzed together and enhance overall accuracies within wetland mapping activities. An example of this combination in a GIS could be field surveys and satellite imagery. The field surveys are able to capture the fine detail present at the ground level and their sampling plots can be precisely determined with GPS but the spatial scale of their study is small and unable to capture the whole wetland (e.g., 10s of metres). Satellite imagery can capture a much greater coverage of the study area (e.g., 10s of Kilometres; the whole wetland) but the fine detail observed by the ground team is lost. The trade off between the fine scale detail (e.g., field survey) and broader spatial coverage (e.g., satellite imagery) highlights a GIS's ability to integrate these two data sources. This integration allows for a more comprehensive and better understanding of wetland functions across

differing spatial scales. Overall, wetland mappings would not have been able to achieve the advancements it has seen within these ecosystems if not for the inclusion of geomatics.

The use of geomatics to advance our understanding is presented in the next chapter, Chapter 2, which investigates the utilization of Remotely Piloted Aerial Systems (RPAS) deployed in 18 high-altitude wetlands spanning across three different subregions within Alberta, Canada. The research aims to determine the ability of RPAS capturing high resolution imagery (e.g., Optical and Multispectral) to classify these wetlands with high accuracy. It discusses the importance of RPAS within the literature and provides a breakdown of the methodologies for data collection, machine learning classification and pattern analysis. Results of a random tree classifier obtained high accuracies and distinguished the relative importance of the various spectral bands, created indices (e.g., NDVI) and the use of a digital surface model (DSM) for precise vegetation mapping. Validation of the classification compared to the in-situ surveys provide more insight into the challenges associated with wetland mapping. The research also identified several vegetation patterns, using landscape metrics, that varied across an elevation gradient. Overall, the chapter illustrates how RPAS data can provide detailed wetland mapping and the relative importance of different types of data to successful wetland vegetation classification.

Following Chapter 2, the thesis concludes with Chapter 3, which describes how wetlands have been mapped in Canada. It discusses the creation and application of the Canadian Wetland Classification System, the main way of classifying wetlands in the country. The chapter also observes how wetlands are mapped at the national level by the Federal Government of Canada. Since the 18 wetlands analyzed for this thesis are in Alberta, it also highlights the Alberta Wetland Classification System (AWCS) used by the province. I provide insight into why these high-altitude wetlands have not been previously mapped. Lastly, there is observation to additional inventory accuracies for peatland mapping in Canada across the literature using the search term (“Peatland” AND “Mapping”) and limited to research conducted within Canada.

Chapter 2: Assessment of remotely piloted aircraft data classification of wetland vegetation communities and changes in their pattern with elevation

1.0 Introduction

Given the disproportionate contribution of ecosystem services provided by wetlands relative to their global area, wetland mapping has been and remains relevant for both science and society (e.g., Zhang et al., 2010; Fickas et al., 2016). Wetland mapping can be used to aid policy decisions about their protection (e.g., Fang et al., 2016; Xing and Niu, 2019; Valencia et al., 2022) and restoration (e.g., Harvey et al., 2019; Feagin et al., 2020; White et al., 2020) as well as their removal (e.g., Mitsch et al., 1983). Therefore, state/provincial and national government agencies as well as international organizations (e.g., RAMSAR) map, curate, and maintain spatial data of wetland locations within their jurisdictions.

While the location (e.g., Munoz et al., 2009) and boundary (e.g., Adams et al., 1987; Prisley et al., 2020) of wetlands are frequently mapped, less frequent is the quantification and mapping of their ecosystem function. Functional representation and measurement of wetlands is necessary to understand and quantify wetland health and the myriad of ecosystem services they provide to society. For example, wetlands mitigate flood risk (e.g., Furlan et al., 2021; Medvedev et al., 2020), provide unique habitat for species and increase biodiversity (e.g., Bertacchi et al., 2019; Nguyen et al., 2019; Geng et al., 2020; Alvarez-Vanhard et al., 2020; Zhu et al., 2019), remove pollutants and purify water (e.g., Allende et al., 2011), and store carbon (e.g., Mitsch et al., 2013; Gleason et al., 2009) among other services (e.g., Gandarillas et al., 2016). However, the performance of these and other wetland functions is affected by the composition and configuration of vegetation communities within a wetland catchment (e.g., Kelly et al., 2011).

Mapping and quantifying the composition and configuration of vegetation communities has typically been done using in-situ measurements and in some cases by remote sensing. In-situ measurements are often taken along a transect, among a series of plots (quadrats), or some combination of the two (e.g., Wikum and Shanholtzer 1978; Yu and Guo., 2021;). While these methods have been widely used and have been essential to our understanding of

ecology, repeated sampling can negatively impact the natural wetland system by trampling fragile local fauna (e.g., Kalacska et al., 2013) and local wildlife can be disturbed by path generation that can increase exposure to predators or cause nest abandonment (e.g., Carney and Sydeman, 1999; Francis et al., 2020). Despite the benefits and desire for detailed in-situ data, labour, time, and cost constraints inhibit the deployment of in-situ measurements across large spatial extents.

When in-situ data are paired with remotely sensed data, field measurements can be used to calibrate (e.g., Holden et al., 2021) and validate (e.g., He et al., 2019) manual or automated classifications of wetland characteristics. Through this relationship, remotely sensed data offer the ability to scale out in-situ data collection to map wetlands across large spatial extents (e.g., Alvarez-Vanhard et al., 2020). This approach has been used to map wetland boundaries (e.g., Mui et al., 2015), their change over time (e.g., Baker et al., 2007), surface water (e.g., Mueller et al., 2016), estimate vegetation biomass (e.g., Mutanga et al., 2012), and map land use and land cover change leading to wetland loss (e.g., Dewan and Yamaguchi, 2009). While satellite-based data has advanced our ability to map wetland presence and their boundaries, their catchments, and their change over time across larger spatial extents, satellite sensors have not yielded the fine resolution (<5 centimeters) required to quantify the composition and configuration of wetland vegetation communities.

The ability to obtain very fine resolution remotely sensed data is now achievable using contemporary remotely piloted aircraft (RPA; e.g., Nguyen et al., 2019; Ancin-Murguzur et al., 2020). RPA can collect data across meso-scale spatial extents (e.g., 100s ha; Helm et al., 2020) covering more area than in-situ plots (e.g., cumulatively 10s of m^2; Pérez-Ortiz et al., 2015) at a resolution not yet achievable by satellite and mid-altitude airborne data acquisition (although new constellations are closing the gap; e.g., Planet 10 cm; Albedo Space, 2023). Additional benefits of RPA over satellite data acquisition are that RPA can be deployed on-demand at relatively low cost (e.g., Flores-de-Santiago et al., 2020; Dale et al., 2020) to correspond with field data collection, are minimally affected by atmospheric conditions or cloud cover, and are flexible in their deployment to accommodate the acquisition of data at different spatial and temporal resolutions. The combination of 1-2cm resolution from multiple sensors (e.g., optical, multi-spectral, infra-red, thermal, and LiDAR) with in-situ measurements enables advancements beyond mapping wetland presence and boundaries to mapping and

quantifying the composition and configuration of vegetation communities that comprise the wetland. Despite this capability, very high resolution (1-2cm) wetland vegetation community and species has been limited to *Phragmites austrailis* and *Myriophyllim aquaticum* (Bertacchi et al., 2019), coastal marsh dominated by *Spartina patens* (Broussard III et al., 2020), and swamp and non-swamp vegetation and subspecies using LiDAR (Banerjee et al., 2019).

As a step toward filling the gap in our understanding about the composition and configuration of wetland vegetation communities, we systematically evaluate the combination of different data layers generated from RPA flights to map vegetation composition and configuration. We focus on high-altitude wetlands that have been excluded from Canadian Wetland Classification System (CWCS) mapping and are typically void from the literature. Through this effort we seek to determine the following: what is the relative contribution of different data types on the accuracy of RPA wetland vegetation community classification as conducted through object-based image analysis and how does this classification compare to in-situ measurements? To what extent does the composition and configuration of wetland vegetation communities drive RPA classification accuracy? And how does the composition and configuration of wetland vegetation communities change among natural regions or along a gradient in elevation?

2.0 Methods

2.1 Study Area

Within Canada there are roughly 1.29 million Km^2 of wetlands covering an estimated 13% of the country's terrestrial surface (National Wetlands Working Group, 1997). However, these estimates and the types of data used to generate them (e.g., Canadian Wetland Classification System (CWCS); Rubec, 2018) have limitations and omissions. Our study area comprises a set of wetlands that lie within the Subalpine, Montane, and Upper Foothills natural subregions of Alberta, Canada, that have not been previously mapped in the CWCS, Alberta Biodiversity Monitoring Institute (ABMI), documented by Ducks Unlimited, or made available for public access (Ilyas 2022). Within these subregions, a total of 18 sites, between 1415-2106m ASL, covering roughly 0.59 Km^2 were surveyed using RPA and contained in-situ field measurements (Figure **1**; Appendix A). While the Alberta Wetland Classification System

(Alberta Environment and Sustainable Resource Development (ESRD), 2015) would classify all 18 sites as peatlands, the composition and configuration of their vegetation and annual inundation are variable.

All study sites lie within Alberta's Division No. 15, which covers 28,403 Km^2 area with an estimated population of 38,594 in 2016 (Statistics Canada, 2016). Given the low population density, human disturbance in the study region is relatively low; however, the region is actively used for recreation, cattle grazing, and logging (Public Lands Act, 2000; Bow River Basin Council, 2021). Our study sites were selected to best represent areas that had minimal anthropogenic disturbance, but also were in proximity to roadways for access.

The three subregions experience variable temperature and precipitation. The subalpine subregion has a mean annual temperature of -0.1°C and typically receives 755mm of precipitation annually with 56% falling during the growing season. The montane subregion has a mean annual temperature of 2.3°C and typically receives 589mm of precipitation annually with 65% falling during growing season. The upper foothills subregion has a mean annual temperature of -1.3°C and typically receives 632mm of precipitation annually with 71% falling during growing season (Natural Regions Committee, 2006).

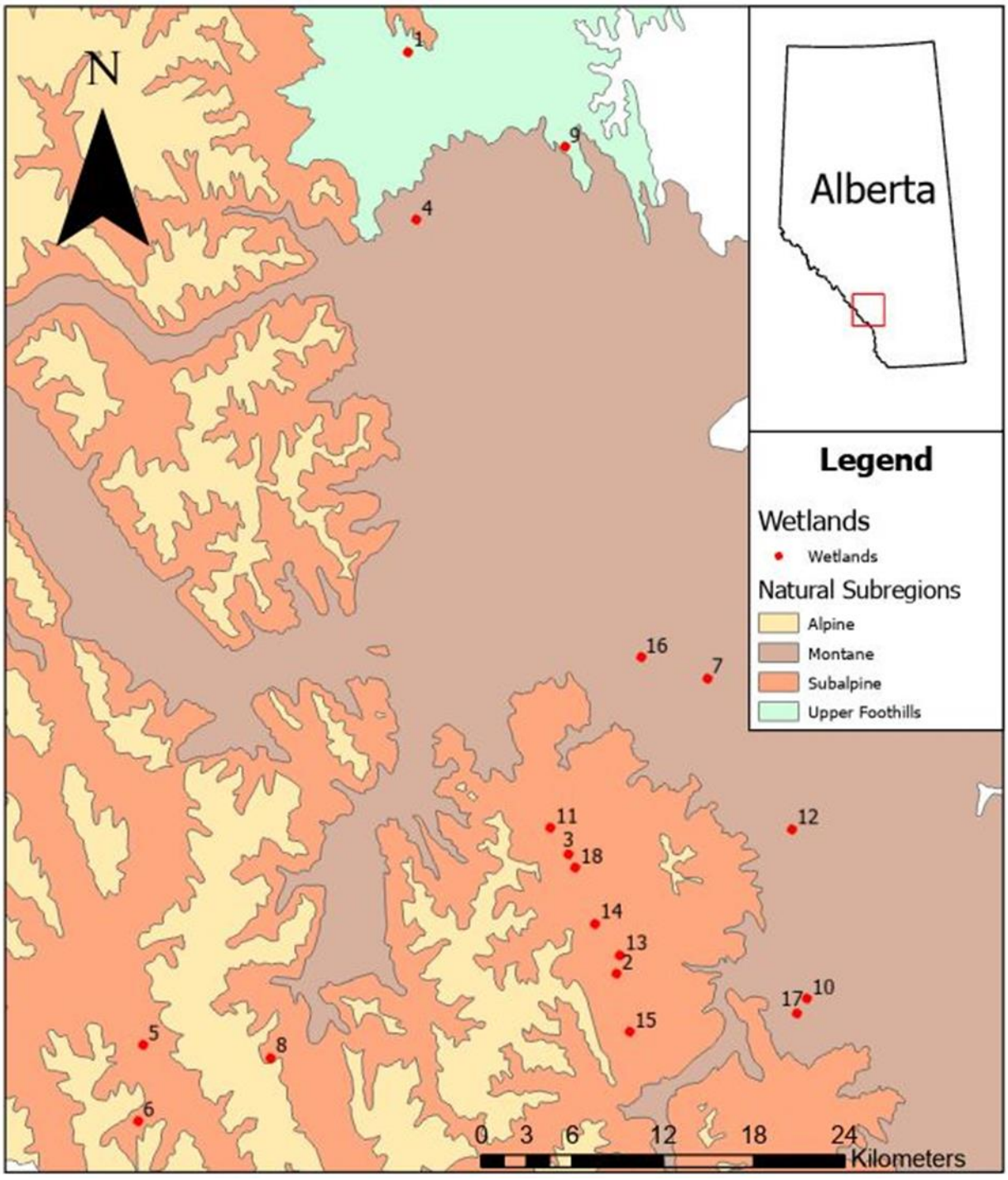


Figure 1: Study area showcasing 18 study site wetlands flown via RPAS with the natural subregions with the area of interest (Numbers correspond to the Site No. provided in Table 2)

2.2 Data

2.2.1 RPA Survey and Data Creation

Each of the 18 study sites were flown using a Da-Jiang Innovations (DJI) Inspire 1 remotely piloted aircraft (RPA). The Inspire 1, a quadcopter, was equipped with a Zenmuse Z3 optical camera and a Parrot Sequoia multi-spectral camera. The Zenmuse Z3 is a complementary metal oxide semiconductor (CMOS) optical sensor able to capture the visible light spectrum (Red, Green, Blue wavelengths) to create 12-megapixel images. The Parrot Sequoia (SenseFly, Cheseaux-sur-Lausanne, Switzerland) is a multispectral sensor and optical camera. It captures 4 bands; Green (550nm +/- 40nm), Red (660nm +/- 40nm), Red edge (735nm +/- 10nm) and Near infrared (790nm +/- 40nm). The optical camera (RGB) captures 16 megapixel photographs. With both sensors installed, the Inspire 1, had a total weight of 3.37 kg and a maximum flight time of 18 minutes.

To ensure flight safety for complete wetland coverage flights were conducted at 60 m AGL, which yielded a spatial resolution of approximately 2.5 cm for the Zenmuse and 6.3 cm for the Sequoia. This flight covered the entire area of the study site. Prior to each flight, ground control points (GCPs) were deployed around the study site to georeference RPA data for horizontal and vertical measurements. The number of GCPs (10-18) varied from site to site depending on the size of the site and accessibility. GCP placements were around each site's perimeter with some lain within their inner region. Each GCP was a 12" x 12" checkered vinyl floor tile with a distinct center point delineated by high contrast of black and white ¼ section squares. The location of each GCP was recorded using a Leica Viva GS14 GNSS rover with a Leica Viva CS15 field controller and a second Leica GS14 GNSS base station, which were able to achieve an average accuracy of 5cm or less.

RPA acquired imagery were processed using Pix4D (Pix4D SA, Switzerland) and structure-from-motion, along with GCP locations, to generate ortho-mosaics of different sensor returns as well as a digital surface model (DSM) for each field site. An orthomosaic was generated for the Zenuse optical sensor and each band of the Sequoia (i.e., green, red, red edge, near-infrared).

While only six types of data were acquired from the RPA and structure-from-motion process, these data were used in different combinations to generate spectral indices to

facilitate the differentiation of vegetation communities (e.g., Beyer at al., 2019; Sharma, 2022). Prior to the generation of these indices all RPA data were georeferenced and partitioned (i.e., clipped) to the same areal extent using PyCharm Community Edition 2022.1.3 (JetBrains s.r.o., Czech Republic) and within ArcGIS (ESRI, California, United States). Spectral indices were generated using Trimble's eCognition Developer v.10.3 (Munich, Germany) software and included: Normalized Difference Vegetation Index (NDVI), Red Edge Chlorophyll Vegetation Index (RECI), Normalized Difference Red Edge Vegetation Index (NDRE), Green Normalized Difference Vegetation Index (GNDVI), Green-Red Vegetation Index (GRVI) Normalized Difference Water Index (NDWI), Soil Adjusted Vegetation Index (SAVI), Optimized Soil Adjusted Vegetation Index (OSAVI) and Green Chlorophyll Vegetation Index (GCI).

2.2.2 In-situ survey

Within each of the 18 locations studied a combination of quadrats and transects were used for in-situ survey measurements. Transects were 50 m in length and spaced roughly 50 m away in parallel to each other. Five 1 x 1 m quadrats were equally spaced along each transect. The location of the middle of each quadrat was acquired using the aforementioned Leica Viva GS14 GNSS rover. Vegetation within each quadrat was identified by species type and the total amount present as a percent of quadrat area. In the case that canopy cover was present over top of a quadrat, both the understory and canopy vegetation were identified and were included in the overall percent composition (Iljas, 2022). A dominant vegetation community was assigned to each quadrat based on the composition of vegetation communities within (Table **1**).

Table 1: Classification of quadrats based on ground sampling of vegetation composition (Iljas, 2022)

Type	Composition
Grass	If <15% shrubs and >40% grass, then grass If >50% grass + litter, and grass is at least 20%, then grass
Litter	If >60% littler and not >30% grass or >15% shrub, then litter
Mixed Shrub	If >15% shrub and no more than ~20% anything else, then mixed shrub
Moss	If >15% shrubs and >40% moss, then moss
Shrub	If > 40% shrubs, then shrub
Water	If >50% open water and <~20% shrubs, then water

2.3 Object-Based Image Analysis (OBIA) with eCogition

2.3.1 Automated Vegetation Community Classification

An object-based image analysis (OBIA) was performed on each of the 18 study sites using eCognition Developer (Trimble 2019. eCognition Developer). The OBIA is composed of several steps (segmentation, training site delineation, segment classification, and post classification; e.g., Thiel et al., 2020; Paudel et al., 2021). In the segmentation step, objects are created that comprise a collection of pixels that are grouped together based of similar pixel characteristics or pixel values to create polygon objects that are used to identify features in a landscape. A multi-resolution segmentation process was applied, which is a bottom-up approach that uses a pairwise region merge to create objects based on the average heterogeneity at the pixel level (Trimble, 2022). The multi-resolution segmentation process takes a single pixel within the imagery and pairs it with neighbouring pixels through several iterations based off of their collective overall shape and spectral characteristics. If a neighbouring pixel is not a candidate then the process for the object is stopped and a new routine proceeds to form the next object. The process is repeated until each pixel within the imagery has been assigned to an object.

The final segmentation parameters that were applied to all 18 study sties were derived by systematically varying the scale (10 - 100), compactness (0.1 - 0.9), and shape (0.1 - 0.9) parameters for four of the study sites until segments did not incorporate more than one vegetation community type, segments corresponded to small patches of vegetation, and they could be aggregated to delineate large patches of the same vegetation community. The shape parameter describes the relationship between the spatial form of the segment and its colour since the overall homogeneity of a segment is a function of the spectral values of the pixels within (Trimble, 2022). The compactness parameter influences the degree to which segments can have long perimeters with small areas or inhibits the degree to which they can deviate from a standard geometric shape (e.g., circle) (Trimble, 2022). The multi-resolution segmentation used for this project had a scale factor of 60, a shape factor of 0.1 and a compactness factor of 0.9.

2.3.2 Training Site Selection

Training sites comprise a selection of samples from imagery for each wetland study site; these selected samples represented the classes of interest (11 classes total; Table **2**) used to train a Random Tree classification algorithm. Training sites were manually identified by selecting segmentation objects that completely contained only the vegetation or land cover class of interest. We sought to conform to recommendations for 10-30n training samples, where n is the number of spectral bands used within the imagery (e.g., Mather 1999; Park & Stenstrom, 2008). With the 5 bands captured by our UAV data collection (i.e., Red, Blue, Green, NIR and RE) the total number of samples for each class ranged from 50 (10n, n= 5) to 150 (30n, n=5). Instances occurred where the homogenous similarity of vegetation colours produced smaller and more abundant (fragmented) objects that an upward of 500 samples were collected. In other situations, it was not possible to obtain the recommended sample count given the limited presence of a vegetation or land cover type. When this occurred (litter, snag, dirt/ground, or rocks), approximately 75% of the segments visually identified as those types within a wetland study site were selected. Across all wetlands (n = 18), a total of 13948 samples were collected.

Table 2: Vegetation and land cover classes for classification

Type	Traits
Grass	Long narrow strands (i.e., blades), ranged from light yellow to green in colour
Dirt/ Bare ground	Areas without any vegetation, generally varying shades of brown in colour
Litter	Dead, fallen trees. Generally, tree trunks white to light grey in colour
Moss	Flat patches of vegetation with little to no vertical structure. Generally light yellow to light brown in colour
Mixed Vegetation	Combination of grasses and different types of shrubs; ranged from light to dark green in colour
Rock	Grey irregular features with sharp corners. Found isolated and grouped together
Shadow	Dark (black) features protruding off tall features (i.e., trees) due to the angle of the sun
Shrub	Mid-sized, circular vegetation patches resembling a bush. Colours ranged in varying shades of green
Snag	Standing dead trees; white to light grey in colour. Visible branches without canopy cover or leaves
Tree	Standing trees (>2m height) with visible canopy present; dark green in colour. Includes a combination of coniferous and deciduous tree
Water	Water features including channels and streams; generally blue and navy in colour

2.3.3 Random Tree Classifier

A Random Tree Classifier is a type of machine learning classifier that can be used to classify segmented objects into wetland vegetation and land cover (e.g., Amani et al., 2017). A Random Tree comprises a collection of predictions from multiple decision trees that collectively assign a class to a segmentation object (Breiman, 2001). Each “tree” casts a vote based on the training samples (i.e., training sites) and the class which receives the most votes overall is assigned (e.g., Lorena et al., 2011). When enough “trees” are generated, the resulting product is known as Random Forest (Breiman, 2001). Through this process, RT reduces the chances of overfitting and increases the overall performance of the classifier, particularly when working with noisy data or imagery containing similar spectral characteristics (e.g., Van Hulse and Koshgoftaar, 2009; Immitzer et al., 2012).

The [Random Tree] classifier’s training parameters for this study used a combination of both image layers and object features. The image layers used mean values of the pixels within each object and included DSM, GCI, GNDVI, GRVI, NDVI, NDWI, OSAVI, RECI, SAVI, Blue, Green and Red. Differing from the pixel summarization conducted with the image layers, object features describe the characteristics of the objects themselves for which object compactness, density, rectangular fit, roundness and shape index were used. Additional Random Tree classifier parameters included the maximum number of categories (i.e., branches, 20), active variables (i.e., image layers and object features; 15), maximum number of trees (125) and forest accuracy (0.01). The “Max categories” parameter limits the number of categories that a tree can grow (i.e., number of branches per tree). Without this limitation, the tree can grow with many branches to overfit the data. The maximum number of trees limits the total number of trees generated by the classifier and forest accuracy identifies the required minimum accuracy threshold that needs to be met prior to training completion.

2.4 Accuracy Assessment

To assess the accuracy of wetland vegetation community and land cover classification, two approaches were used. The first involved a comparison of classification results against a subset of training samples excluded from the classification process, facilitated by eCognition’s Accuracy assessment. This was conducted for all 18 wetlands and

used a traditional confusion matrix approach (e.g., Congalton, 1991) that provides an overall accuracy (OA), user's Accuracy (UA), and producer's Accuracy (PA).

The user's accuracy (UA), also known as the accuracy of omission, refers to the frequency that mapped classes are present on the ground but not accounted for in the classification. UA identifies the percentage of correctly classified objects relative to the number of objects that belong to that class and is calculated by dividing a class's correct classification by its row total to represent the classification's reliability. Complementing the UA is the producer's Accuracy (PA), also known as the accuracy of commission, which refers to the frequency that real features on the ground are correctly shown on the classified map. PA identifies the percentage of correctly classified objects relative to the total number of objects that truly belong to that class and is calculated by dividing the number of objects that were correctly classified by the total number of test sites for that class.

The second accuracy assessment approach compared the classified results to in-situ field measurements, using a similar confusion matrix approach. Each wetland contained a series of 0.5x0.5 m plots arranged 50m apart along 3 transects. Within each plot, the dominant vegetation was recorded. A total of 169 geolocated plot centroids, established with a Leica GS14 and Leica Viva CS15 field controller (horizontal accuracy of 5cm or less) (Illyas 2022), were used in our field-based accuracy assessment. The orientation of the plots was not recorded, therefore if plots were visible in imagery (due to temporal correspondence) then they were manually digitized (n = 35). If plots were not visible in imagery then plot-centroids were buffered by 0.5m and then enveloped to a squared polygon to simulate the same quadrat size used for each plot (n = 117, ArcGIS Pro – Buffer, 2023; ArcGIS Pro – Feature Envelope to Polygon, 2023).

3.0 Results

3.1 Accuracy Classification against training samples

An accuracy assessment for each classified wetland was calculated within eCognition using a subset of input samples (i.e., training sites). Overall accuracy varied among our 18 wetland sites from 83.7-98.4%, with a total overall average accuracy of 91.43% (Table **3**).

Table 3: Surveyed locations sorted by elevation (Includes Site Number, Natural Subregion, Municipality, Elevation and Overall Accuracy)

Elevation (m)	Natural Subregion	Municipality	Location	Site No.	OA
1419	Montane	Kananaskis	659762 E, 5647083 N	7	91.2%
1465	Montane	Kananaskis	653898 E, 5656884 N	12	86.4%
1478	Montane	Big Horn No.8	661067 E, 5635918 N	9	85.6%
1489	Montane	Kananaskis	645071 E, 5645065 N	16	88.5%
1504	Montane	Kananaskis	643536 E, 5691652 N	10	83.7%
1522	Montane	Kananaskis	633036 E, 5697663 N	17	92.0%
1559	Montane	Big Horn No.8	649418 E, 5633384 N	4	90.1%
1572	Upper foothills	Big Horn No.8	645550 E, 5644129 N	1	98.3%
1697	Subalpine	Kananaskis	617124 E, 5626644 N	13	94.3%
1718	Subalpine	Big Horn No.8	660468 E, 5634966 N	2	98.4%
1739	Subalpine	Kananaskis	633879 E, 5686575 N	15	84.4%
1744	Subalpine	Kananaskis	625765 E, 5631100 N	11	96.0%
1795	Subalpine	Kananaskis	617310 E, 5631688 N	14	92.4%
1800	Subalpine	Kananaskis	648468 E, 5637200 N	18	94.9%
1839	Subalpine	Kananaskis	646946 E, 5640492 N	5	88.8%
1844	Subalpine	Kananaskis	649481 E, 5658101 N	3	93.8%
1962	Subalpine	Kananaskis	648654 E, 5638460 N	6	96.8%
2106	Subalpine	Kananaskis	643833 E, 5646726 N	8	90.1%
					Total Overall Average: 91.4%

The overall user's accuracy (UA) average of all classified classes was 92.7% with an average standard deviation of 7.7%. The obtained UA (mean) values ranged from 81.3% to 98.0% and their respective standard deviations ranged from 4.0% to 16% (Table **4**). User's accuracy for Litter (12%), Rock (16%) and Water (12%) were the only classes that obtained a standard deviation > 10%, which is primarily due to the limited presence of these classes. The most accurately classified vegetation and land cover classes were Tree, Moss, Ground/Dirt, and Shadow, which obtained mean UAs greater than 95% and had standard deviations of 4%, 4%, 5%, and 2%, respectively.

The overall producer's accuracy average of all classified classes was 86.9% with an average standard deviation of 12.7%. Individual wetland average PA values ranged from 63.4% – 97.9%, with average standard deviation ranging from 2% – 28% (Table **4**). The least accurate classes for producer's accuracy were Moss and Snag with 78.4% and 63.8% and had a mean standard deviation of 27% and 28%, respectively. All remaining classes obtained mean producer's accuracy results greater than 80% with Rock (97.0%) and Shadow (97.9%) achieving the highest PA. Of the classes that obtained PA mean values greater than 80%, Grass, Litter, Shrub and Water also had relatively high average PA standard deviations (>10%). Similar to the UA outcomes, the larger standard deviations are primarily due to the limited presence of those classes within several wetlands. Visual inspection of wetland classifications qualitatively verified that wetlands with a higher presence of a class and were able to obtain the minimum sample count (10n), achieved higher PA values with lower standard deviations. This was best represented by the following classes: Mixed Vegetation (92.5%, 0.06), Tree (92.4%, 0.06), Ground/Dirt (93.3%, 0.06), Rock (97.0%, 0.05), Shadow (97.9%, 0.02)

A PA > UA signifies that the classification has overestimated what is present on the ground. Two classes (Mixed Veg and Rock) both obtained mean PA values greater than mean UA values. Mixed Vegetation mean PA value shows that 92.5% of the classification has been correctly identified as Mixed Vegetation but its mean UA value of 87.5% highlights the true amount of this class's presence on the ground as correct. The same was observed with the Rock class which obtained a mean PA value of 97.0% but a mean UA value of 81.3%. The remaining 9 classes (Grass, Ground/Dirt, Litter, Moss, Shadow, Shrub, Snag, Tree and Water) all obtained mean UA values greater than their complementary mean PA values, which

highlights that the classification has underestimated these classes across the wetlands and that the true reality of the classes [correct] presence on the ground is higher than what was classified.

Table 4: Summary of user's and producer's accuracy for all classified wetlands (including average and standard deviation)

Class	**UA range**	**UA_m**	**UA_{sd}**	**PA range**	**PA_m**	**PA_{sd}**
Grass	73.4 – 100%	91.1%	0.09	62.0 – 95.8%	81.5%	0.12
Ground/Dirt	86.7 – 100%	97.7%	0.05	85.7 – 100%	93.3%	0.06
Litter	68.4 – 100%	93.2%	0.12	62.5 – 100%	86.0%	0.13
Moss	89.4- 100%	95.6%	0.04	11.8 – 100%	78.4%	0.27
Mixed Veg	74.1 – 100%	87.5%	0.08	79.5 – 99.5%	92.5%	0.06
Rock	66.7 – 100%	81.3%	0.16	88.9 – 100%	97.0%	0.05
Shadow	94.7 – 100%	98.0%	0.02	94.5 – 100%	97.9%	0.02
Shrub	76.7 – 97.1%	90.7%	0.07	53.3 – 100%	85.8%	0.14
Snag	84.6 – 100%	94.5%	0.06	16.7 – 100%	63.4%	0.28
Tree	88.7 – 100%	95.2%	0.04	79.7 – 100%	92.4%	0.06
Water	60.0 – 100%	95.3%	0.12	21.4 – 100%	87.9%	0.21

3.2 Image Layer and Object Feature Importance for Random Tree Training

Results from the RT classifier were interrogated to identify the importance or influence of each image layer and object feature on the classification of each study site wetland. The twelve image layers (Section 2.3.3.4) had an importance weight ranging from 2.3% – 30.8% and standard deviations ranging from 1.0% – 6.4% (Table **5**). The image layer with the greatest overall importance was the Digital Surface Model (DSM), which had with an average weight of 15.9% and an average standard deviation of 6.4% across the 18 study sites. The image bands were the next most important contributors to the classification with mean R, G, B weighted. This was followed by mR, mG and mB which had importance weights of 8.9%,

8.7% and 7.4%, respectively. The remaining created index layers received lower average weights; mGRVI (6.3%), mRECI (5.2%), mNDWI (5.1%), mGCI (4.9%), mGNDVI (4.9%), mSAVI (4.5%), and mNDVI and mOSAVI both with 4.4% weighted importance. Across all 18 study sites, the five object features had an importance weight ranging from 1.8 – 9.3%. And a standard deviation ranging from 0.8 – 1.9%. The highest average weighted object feature across all 18 study sites was Shape index with an average weight of 4.6% followed by Density (3.9%), Roundness (3.7%), and Compactness and Rectangular fit both returning 3.6%. Importance values provide two key insights about the classification of wetland vegetation communities using very high-resolution data. First, these values demonstrate that image layers (individually and collectively) played a larger role in the classification than object features. The overall average of all imager layer weights combined was 6.7% with an average standard deviation of 2.4% and the overall average of all object feature weights was 3.9% with an average standard deviation of 1.1%. Second, in lieu of a canopy height model, the DSM had twice the importance of spectral layers (e.g., blue, green, red) and indices comprising their combination. This last point suggests a critical role that the representation of three-dimensional wetland catchments can have on understanding vegetation composition and configuration as well as the importance of structure-from-motion multi-view stereo (SfM-MVS) approaches when LiDAR data are unavailable.

Table 5: Weighted importance of each layer used to train the RT classifier (Includes average and standard deviation)

Site No. / Layer	mDSM	mGCI	mGNDVI	mGRVI	mNDVI	mNDWI	mOSAVI	mRECI	mSAVI	mB	mG	mR	compactness	Density	Rectangular fit	Roundness	Shape Index
No. 1	10.2%	6.4%	7.1%	6.3%	5.0%	7.1%	4.9%	4.9%	4.7%	6.0%	7.2%	6.5%	4.4%	4.4%	4.3%	4.3%	6.1%
No. 2	8.3%	5.4%	5.3%	6.4%	5.6%	5.3%	5.7%	5.4%	5.7%	6.0%	6.7%	5.4%	5.0%	5.6%	4.8%	5.1%	8.3%
No. 3	30.8%	2.3%	2.3%	2.3%	2.3%	2.3%	2.3%	2.3%	2.3%	10.1%	13.7%	13.1%	2.7%	2.8%	3.2%	2.4%	2.9%
No. 4	13.5%	5.4%	4.4%	13.4%	4.3%	4.4%	4.5%	5.4%	4.3%	5.3%	5.8%	4.6%	3.8%	3.9%	3.9%	3.7%	9.3%
No. 5	20.5%	4.3%	3.9%	5.0%	4.8%	4.2%	5.2%	5.2%	4.9%	7.7%	7.8%	6.7%	3.8%	3.9%	4.0%	3.8%	4.4%
No. 6	11.7%	10.1%	7.9%	4.8%	4.0%	9.5%	3.9%	4.2%	4.0%	6.8%	8.2%	6.6%	3.9%	3.5%	3.4%	3.6%	3.7%
No. 7	18.2%	4.0%	4.0%	4.9%	4.5%	3.8%	4.5%	5.5%	4.7%	8.7%	7.1%	11.2%	3.7%	3.8%	3.7%	3.7%	3.9%
No. 8	8.4%	6.8%	8.4%	4.5%	3.9%	11.1%	4.0%	4.1%	4.0%	8.1%	7.6%	8.1%	3.8%	4.5%	3.8%	3.9%	4.8%
No. 9	12.9%	4.4%	3.9%	5.7%	5.3%	4.2%	5.2%	5.3%	5.2%	10.6%	10.5%	7.2%	3.7%	3.7%	3.8%	3.6%	4.8%
No. 10	12.6%	6.0%	6.6%	6.7%	3.7%	6.5%	3.7%	4.2%	3.5%	10.2%	13.4%	5.1%	3.5%	3.5%	3.6%	3.4%	3.8%
No. 11	20.4%	4.7%	4.7%	8.8%	4.1%	4.8%	4.1%	4.1%	4.1%	5.6%	10.0%	8.4%	3.3%	3.1%	3.2%	3.3%	3.4%
No. 12	16.4%	4.5%	4.3%	4.3%	4.2%	4.3%	4.3%	4.6%	4.3%	6.5%	7.2%	10.5%	4.0%	6.0%	4.2%	5.5%	4.9%
No. 13	10.9%	2.3%	3.0%	14.2%	8.7%	2.8%	6.8%	9.6%	7.9%	4.9%	5.9%	13.3%	2.1%	2.0%	1.8%	2.0%	1.8%
No. 14	25.9%	2.9%	3.1%	5.3%	3.2%	3.0%	3.9%	11.2%	3.9%	5.0%	8.2%	12.9%	2.2%	2.5%	2.2%	2.2%	2.4%
No. 15	21.9%	3.9%	4.5%	4.3%	3.4%	4.4%	3.5%	3.6%	3.4%	3.6%	10.8%	17.8%	2.9%	3.2%	3.1%	2.8%	2.9%
No. 16	20.1%	4.2%	4.2%	4.9%	4.2%	4.2%	4.2%	4.2%	4.2%	8.7%	7.0%	8.4%	4.3%	4.3%	4.3%	4.2%	4.3%
No. 17	8.3%	5.5%	5.3%	5.8%	4.3%	5.1%	4.3%	4.4%	4.3%	8.5%	11.1%	7.8%	4.5%	5.5%	4.6%	4.5%	6.2%
No. 18	14.9%	5.4%	5.4%	5.2%	4.4%	5.1%	4.6%	5.4%	4.6%	10.4%	8.1%	7.2%	3.8%	3.9%	3.6%	3.8%	4.4%
Low	8.30%	2.30%	2.30%	2.30%	2.30%	2.30%	2.30%	2.30%	2.30%	3.60%	5.80%	4.60%	2.10%	2.00%	1.80%	2.00%	1.80%
High	30.8%	10.1%	8.4%	14.2%	8.7%	11.1%	6.8%	11.2%	7.9%	10.6%	13.7%	17.8%	5.0%	6.0%	4.8%	5.5%	9.3%
Average	15.9%	4.9%	4.9%	6.3%	4.4%	5.1%	4.4%	5.2%	4.5%	7.4%	8.7%	8.9%	3.6%	3.9%	3.6%	3.7%	4.6%
Std	6.4%	1.8%	1.7%	3.0%	1.3%	2.2%	1.0%	2.1%	1.1%	2.1%	2.4%	3.5%	0.8%	1.1%	0.8%	0.9%	1.9%

3.3 Comparison of Ground Survey and RPA Classification

Evaluation of RPA data classification accuracy against in-situ measurements required a reduced number of classes since Litter, Snag, Dirt/Bare ground, Rock, and Water had an insufficient number of training sites in the RPA data or were absent from in-situ plots (e.g., snag, Dirt/Bare ground, Shadow). Furthermore, Broadleaf was not independently discernable from the RPA data and was subsequently aggregated with the Mixed Vegetation class. A total of 152 quadrats (n=152) were analyzed, user's accuracy and producer's accuracy were 58.1% and 47.4% respectively with an Overall Accuracy of 54.5% (Table **6**). The most accurate classes were Shrubs (76.0%) followed by Grass (61.9%), Moss (58.3%) and Mixed Vegetation (36.3%). The PA values highlight the models fair accuracy at classifying the Shrub, Grass and Moss classes but are not able to accurately classify Mixed Vegetation. With observation to Mixed Vegetation, the number of correct classifications (n = 33) compared to the total number of classifications (n = 91) shows that this class was overestimated within the imagery. The opposite occurred for Moss which obtained a high PA value (58.3%) but only had 7 correct classifications with a total of 12 classifications highlighting how this class was underestimated. Also, of the 12 wetlands used for the in-situ ground survey comparison, only subalpine (n = 7) and montane (n=5) were present; the singular wetland in the upper foothills subregion was not included. Overall Accuracy between the subalpine wetlands ranged from 20-73% with an average of 47%. The montane wetlands ranged from 13-40% with an average of 30%.

Table 6: In situ ground survey comparison with removal of classes that did not obtain a minimum sample size of 50 and aggregation of Broadleaf into Mixed Vegetation

RPAS Class							
Ground Survey Classification		Shrubs	Grass	Mixed Veg	Moss	Total	User's Accuracy %
	Shrubs	19	3	23	1	46	41.3%
	Grass	0	13	13	2	28	46.4%
	Mixed Veg	2	2	33	3	40	82.5%
	Moss	4	3	22	7	36	19.4%
	Total	25	21	91	12	n = 152	47.4%
	Producer's Accuracy	76.0%	61.9%	36.3%	58.3%	58.1%	OA = 54.5%

Despite the high level of accuracy achieved when the vegetation and land cover classification was assessed relative to the training samples, several classes (Broadleaf, Water, Rock, Litter and Dirt/Bare Ground) from the classification returned [both] user's accuracy and producer's accuracies of 0.00%. These poor results were due to the inability of the RPA data to distinguish the character traits associated with broadleaf vegetation using a 2.4cm resolution orthomosaic, which were similar to the shape and colour of grasses and mixed vegetation. Water and Rock yielded a lack of accuracy due to their lack of presence. For example, Water was present only twice and Rock once in the quadrats and therefore from the imagery used (60m) the rock was not large enough in size to be observed (only surrounding vegetation was identified) and for Water, the classification overestimated the surrounding vegetation along the banks edge. Litter presented an issue when comparing field assessments, the size of the debris (tree remains) was not able to be classified at the same level performed by the field surveying team. At 60m flight height large litter objects were able to be identified and classified while smaller sized objects observed at the ground level could not. For this reason, there was not a singular litter classed correctly compared to in this assessment. Both Shadow and Dirt/Bare Ground were misclassified once through

comparison. Visual observation to the aerial imagery shows that the classification was correct; Shadow is present within the imagery.

3.4 Composition and Configuration

To determine how the composition and configuration of wetland vegetation communities change amongst natural regions or along a gradient in elevation (Objective 4) a wetland boundary delineation was completed to isolate the study area from surrounding manmade features (roads, non-wetland areas) using a 10 m resolution Digital Elevation Model (DEM). Due to the low (coarse) resolution there may be an overestimation in wetland area compared to a higher (finer) resolution DEM (cm level; same resolution as RPA imagery). Similarly, the boundary delineation approach excluded tree cover from upland areas, but tree cover was still observed in the lowland regions of these wetlands. Therefore, using the tree line to delineate wetland boundaries would not be appropriate and could alter the results of pattern metrics. Further refinement to the wetland boundary involved excluding areas with a slope greater than 5 degrees. This exclusion decreased the areal extent of the study wetlands from an average of 0.59 Km^2 to 0.36 Km^2. Without additional data (e.g., hydrological, soil samples) others have shown that a 5-degree slope can be used to delineate wetlands boundary with high accuracy (e.g., Iljas, 2022; Zheng et al., 2017).

The vegetation communities within each wetland were analyzed for their composition and configuration using class and landscape level metrics. A total of 671 landscape metrics were calculated (66 landscape level metrics and 605 class level metrics). However, since landscape metrics are often highly correlated with each other, a pairwise correlation analysis was conducted (in R with the caret Package; Kuhn, 2008; similar to Evans et al. 2017) to reduce these metrics using a cutoff value of 0.75. The pairwise correlation grouped similar metrics and identified the best representative metric by re-evaluating the average correlations from multiple iterations. The cutoff of 0.75 signified a strong correlation and removed 94.8% of the 605 metrics. The remaining 5.2% (35) metrics were regressed against elevation (comprising a range of elevation from 1400m – 2150m) to identify if any variation in the composition and configuration of wetland vegetation communities could be attributed to elevation. Two landscape and three class level metrics were considered statistically significant using a p-value less than $\alpha = 0.05$. The two landscape level metrics (Patch Cohesion Index

(PCI) and Interspersion and Juxtaposition Index (IJI)) can be conceptually classified as aggregation metrics. The three class level metrics belonging to the Mixed Vegetation class were the Coefficient of Variation of Patch Area (Area and edge metric), Coefficient of Variation of Euclidean Nearest-Neighbour distance (aggregation metric) and the number of disjunct core areas (Core area metric).

Patch Cohesion Index (PCI) describes how connected the corresponding patch type is within a landscape. It considers the likelihood of patches being connected to their neighbours and their ability to form large clusters (e.g., Gustafson, 1998). When the distribution of each patch type becomes more clustered (i.e., physically connected) PCI values are high and when the patch types are more dispersed PCI values are low. With increasing elevation patch cohesion values decreased signifying that patch types become less clustered and further dispersed throughout the landscape (Figure **2**a). Interspersion and Juxtaposition Index (IJI) quantifies spatial patterns and arrangements of classes within an area by measuring the amount of mixing (interspersion) and clustering (juxtaposition) of land cover classes. With Values increasing with elevation (Figure 2b). This observation highlights that at lower elevations a class is only adjacent to a few other classes and as elevation increases a class becomes equally adjacent to all other classes.

Coefficient of Variation of Patch Area (CVPA) quantifies patch size variability within a specific land cover class. It measured the dispersion of patches for the Mixed vegetation class within the wetland landscapes. Higher values were present at lower elevations and values decreased with rising elevations (Figure 2c). The presence of high values indicates a larger variation in the Mixed Vegetation patch size. This larger variation suggests there is a non-uniform (heterogenous) distribution of these patches across the landscape at low elevations and with increased elevations the Mixed Vegetation patches become more uniform in their distribution. Coefficient of Variation of Euclidean Nearest Neighbour Distance (CV-ENN) quantifies the variability of distances between neighbouring patches within a specific land cover class. Low values were present at lower elevations and values increased as elevation rose (Figure 2d). The low values indicate a more uniform distribution of the classes patch spacing and higher values indicate a greater variation in the distance between neighbouring patches. As elevation increased, there was a tendency for the distance between neighbouring patches within the Mixed Vegetation class to become more variable and dispersed suggesting

a more heterogeneous distribution of patch spacing. The Number of Disjunct Core Areas (NDCA) quantifies the spatial pattern and fragmentation of core areas by measuring the count of separate or disconnected core areas within a class. High values indicate a division of core areas (fragmented distribution), and low values indicate a more connected or contiguous distribution for Mixed Vegetation patch core areas. The decrease in values as elevation increased indicates the Mixed Vegetation patch core areas become more connected and less fragmented within the wetlands and portrait a more continuous distribution of core areas (Figure 2e).

Plausible ecological explanations for the trends observed with increasing elevation and the five-landscape metrics are due to environmental factors. Environmental factors like temperature, precipitation and soil characteristics change as elevation increases within the subregions of Alberta. With reference to Table 2 and 18 wetlands studied, the montane wetland elevations ranged from 1419m to 1559, the singular upper foothill wetland had an elevation of 1572m, and the subalpine wetlands ranged from 1718m to 2106m. The Montane subregion is the lowest elevated subregion within the Rocky Mountain natural region. Chinooks are common in the montane subregion resulting in warmer winters and lower snowfall totals with milder summer months providing more precipitation (Natural Regions Committee, 2006). Steep slopes and varying levels of wind exposure in the montane subregion create microclimates that vary in vegetation diversity. The Montane is often the driest and warmest of the three subregions observed within this study though it also contains exposed bedrock and unsuitable soils in areas resulting in fewer locations for vegetation growth (Natural Regions Committee, 2006). The Upper Foothills subregion experiences an overall shorter growing season due to its continual cooler climate throughout the year. The Summer seasons are often cool with mild winters and precipitation is high throughout the year with a peak during July (Natural Regions Committee, 2006). The cooler conditions and variable soil compositions within the upper foothills influence lower plant diversity throughout it. (Natural Regions Committee, 2006). Areas with high plant diversity are often accompanied by rich soils and high moisture levels. The opposite is found when plant diversity is low, the area is often drier with poor-nutrient soils. The elevations within the subalpine's differing slope aspects, wind exposure and soil makeup result in varying microclimates (Alberta Parks, 2015). Throughout the majority of the year, the subalpine is cold. With short, wet summers and heavy

snowfall during the winter months, the region experiences the shortest, limited growing season of all subregions observed in this study (Alberta Parks, 2015). At these elevations, ice and snow pellets carried by the wind erode and scrape away at plant tissue (Natural Regions Committee, 2006). Poor soil quality that is low in nutrients paired with increased levels of bedrock overlain with stones produces a low level of plant communities and diversity.

With knowledge of the changing environmental conditions with increasing elevation across these subregions. The further separation and lower levels of clustering of patches present at higher elevations with the Patch Cohesion Index (PCI) suggests there is less available area for vegetation to thrive. Lower temperatures, higher snowfall patterns and increased presence of bedrock material would lead to there being fewer optimal areas that vegetation can remain. With few areas to grow, patch types within these higher elevated landscapes would contain fewer connections to their neighbours and lack the ability to form larger clusters. Like PCI, Interspersion and Juxtaposition (IJI) experiences the same effects from the colder temperatures, increased snowfall, and amount of exposed bedrock. In these higher elevations, there is a lower ability for these patches to mix with one another forming clusters. This is highlighted in the observation that at these higher elevations, the classes become more equally adjacent to all the other classes. In other words, this means there are fewer acceptable growing plots where vegetation could grow resulting in the “salt and pepper” pattern observed. The patterns observed with both Coefficient of Variation of Patch Area (CVPA) and Coefficient of Variation of Euclidean Nearest Neighbour Distance (CV-ENN) due to the increased elevation could be contributed to the soil conditions. At lower elevations, where soil conditions are often higher in nutrients and within a moister environment provide favorable conditions for vegetation growth presenting a higher variability in patch sizes and the less distance between the mixed vegetation patches. Within higher elevated subregions such as the subalpine, soil conditions decrease (i.e., less nutrients and drier) resulting in lower patch size variability and a more dispersed spatial arrangement of the mixed vegetation patches. The Number of Disjunct Cora Areas (NDCA) for the mixed vegetation class becomes more connected and less fragmented at higher elevations signifying a continuous distribution. The Number of Disjunct Cora Areas (NDCA) for the mixed vegetation class become more connected and less fragmented at higher elevations signifying a continuous distribution. Due to the limited availability of locations to grow from the increased exposure of bedrock and

poorer soil quality, the NDCA for mixed vegetation patches have less area to grow. This results in increasing connectedness in the regions they can inhabit. Colder weather temperatures would also inhibit the mixed vegetation patches to congregate in certain areas forming a continuous distribution across the landscape. A potential reasoning for this could be the mixed vegetation patches congregating on the leeward side of these subalpine wetlands to be protected from wind exposure while still providing enough sun exposure.

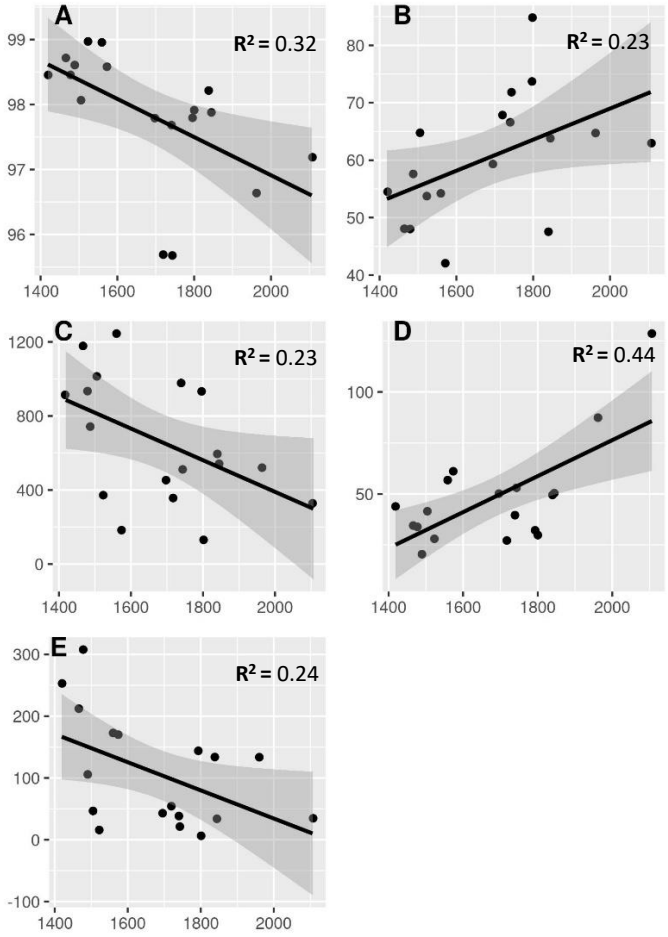


Figure 2: Composition and configuration of both landscape and class metrics that returned statistical significance p lotted against elevation. A) Patch Cohesion Index (PCI) – Landscape Level (p = 0.01), B) Interspersion and Juxtaposition Index (IJI)- Landscape Level (p = 0.04), C) Coefficient of Variation of Patch Area (CVPA) – Class Level (Mixed Vegetation) (p = 0.04), D) Coefficient of Variation of Euclidean NN Distance (CV-ENN) – Class Level (Mixed Vegetation) (p = 0.00), E) Number of Disjunct Core Areas (NDCA) – Class Level (Mixed Vegetation) (p = 0.04)

4.0 Discussion

Remotely piloted aircraft systems (RPAS) are increasingly used to acquire on-demand very-high resolution spatial data. While the equipment used at the time of data collection was state of the art, a reduction in sensor size and improvement in aircraft development is facilitating the collection of subcentimetre and centimetre resolution data from different types of sensors. For example, the ability to acquire 0.005 m resolution optical imagery now facilitates the identification of individual plants (e.g., Torresani et al., 2023); centimetre resolution change detection can quantify changes in topography (e.g., Meinen and Robinson 2020); and LiDAR enables the quantification of plant structure with point cloud densities attainable at 300 points per square meter or greater, among many other scientific applications. However, the use of RPAS for mapping vegetation communities within alpine and sub -alpine wetlands is void from the literature. A literature review of the first 100 results retrieved from the peer-reviewed academic article database Scopus, using a keyword search for “Wetland” AND (“DRONE” OR “RPAS” OR “UAV”) and sorted by relevance, retrieved 57 manuscripts incorporating RPA in wetland research. These manuscripts showcased the use of RPA to delineate streams (e.g., Zweig et al., 2015), map topography (e.g., Pinton et al., 2020; Doughty and Cavanaugh, 2019; Kalacska et al., 2017), determine water surface elevation (e.g., Jiang et al., 2020), as well as their use for monitoring (e.g., Liu et al., 2020; Díaz-Delgado et al., 2019) and restoration purposes (e.g., Harvey et al., 2019; Feagin et al., 2020), observing land use and land cover (LULC) changes (e.g., Kaplan and Avdan, 2018; Pashaei et al., 2020; Canisius et al., 2019; Liu and Abd-Elrahman, 2018; Ciężkowski et al., 2020) through classification (e.g., Geng et al., 2020; Nguyen et al., 2019), and for identifying vegetation species (both domestic and invasive) (e.g., Kentsch et al., 2021; Abeysinghe et al., 2019; Brooks et al., 2019; Bolch et al., 2021; Zhang et al., 2021).

The literature also demonstrates that RPA data acquisition for wetland research is dominated by optical sensors (e.g., Table **7**), which has limited species identification to contrasting plant characteristics such as structural differences (e.g., trees versus shrubs; Kentsch et al. 2021), differences in hue and texture (e.g., phragmites versus myriophyllum aquaticum; Bertachhi et al. 2019), or larger genus (i.e., land cover) type differentiation (e.g., Geng et al. 2020). The literature supports our findings that at a very-fine resolution (~2.5 cm), we are able to accurately classify and map vegetation communities by Genus (Table 6), using an automated

classification approach (overall accuracy ~93%). However, when the classified data were compared to plot level data of those same vegetation types, the plot-level spatial heterogeneity was not captured in the classification, which obtained a substantially lower overall classification accuracy of ~54%. These findings support the utility of RPA data classification for identification and mapping of wetland vegetation communities but cautions that even at very fine centimetre resolution imagery, the ability to accurately map vegetation at the species level may not be possible. Where the authors have been able to map species with high accuracy has occurred where the species are unique relative to other vegetation (e.g., leaf structure), large relative to other vegetation (taller and/or wider), and image resolution has been less than one centimetre (e.g., 0.006 m resolution can accurately identify milkweed plants).

An interesting finding in the literature resides in the lack of understanding about the influence of different independent variables (i.e., feature and object layers) on classification accuracy. In all literature related to the use of remotely piloted aircraft data for wetland vegetation classification and mapping there was no systematic evaluation of the contribution of different inputs on the classification accuracy of different vegetation communities. Understanding the contribution of different drivers of classification accuracy is necessary to determine where future data collection efforts should reside and what types of data and their derivative products are unnecessary.

Table 7: Vegetation classification conducted using remotely piloted aircraft (RPA). NL = Not listed

RPAS (Including Sensor)	Flight Characteristics	Resolution	Class. Type	Vegetation Species	Authors
DJI Phantom 4 Pro, 20 MP, 1-inch sensor (RGB) camera	Altitude = 50m, Overlap = 80%, 90° nadir	1.4 cm	Tidal Flat, Marsh, Upland, Mangrove	*Avicennia germainans* (black mangrove), *Zchizachyrium littorale* (coastal bluestem), *Spartina patens* (gulf cordgrass), *Batis maritima* (pickle weed), *Monanthochloe litoralis* (shoregrass), and *Salicornia spp.* (glasswort)	Nguyen et al., 2019
DJI Mavic Pro, FC220 camera at 90° nadir	Altitude = 105m, Overlap = 80% (Forward) and 65% (Sidelap)	~ 10 cm	Paddy, Exposed Land, Mixed Forest, Mixed Grass, Hyacinth, Lotus, Road-building, Water, Shadow	Uncultivated farmland, River floodplains, Linden, Bamboo, Paliurus, Bermuda grass, Eleusine indica, Paspalum, Road, Wooden trestle, Building, Karst river, Karst lake	Geng et al., 2021
DJI Phantom 4, NL	Altitude = 50m, Overlap = 80%	5-7 cm, NL	Blueberries, Trees, Yellow bushes, Soil, Water, and Dead Trees	Noth American blueberry (*Vaccinium corymbosum x angustifolium*), *Pinus sylvestris* (Trees), *Betula pubescens* and *Betula pendula* (Yellow Bushes)	Kentsch et al., 2021 Cabezas et al., 2020
IRIS Quadcopter, GoPro (12 MP)	Altitude = 5,10 and 25m Overlap = 81% (5m), 66% (10m) and 33% (25m)	0.35 cm (5m), 0.7 cm (10m), 1.75cm (25m),	*Phragmites australis*, *Myriophyllum aquaticum*, *Typha latifolia*, and *Echinochloa crus-galli*	NL	Bertacchi et al., 2018
Trimble UX5, Sony a5100 & Sony NEX-5r	Altitude = 75m, Overlap = 85% (Forward), 80% (Sidelap)	2.33 cm (CIR), 1.95 cm (RGB)	Water, Land (SPPA, PHAU7, Other)	*Spartina patens* (SPPA), *Phragmites australis* (PHAU7), *Bacopa monnieri*, *Pluchea odorata*, *Iva frutescens*, and *Baccharis halimifolia* (Other)	Broussard III et al., 2020)
DJI Inspire 1, Zenmuse X3	Altitude = 100m, Overlap = 70% (Forward), 80% (Sidelap)	1.8 cm	Marginal, Submarginal-subcentral, Central, Flush	Only observed bog ecotopes	Bhatnagar et al., 2020
SenseFly eBee, Parrot Sequoia & Sony DSC WX 220 RGB	Altitude = 120m, Overlap = 75%	3.43 – 13.90 cm	Phragmites, Cattails, Lotus, Lily, and Duckweed	*Phragmites australis*	Abeysinghe et al., 2019
Custom hexa-copter, Phoenix Aerial Scout (LiDAR)	Altitude = 50m, Overlap = NL	7.5 cm	Bare earth, Sedgelands complex, Grass tree, Dagger Hakea, Pouched coral fern, non-swamp	*Empodisma minus*, *Lepidosperma limicola*, *Lepidosperma neesii*, *Leptocarpus tenax*, *Gymnoschoenus sphaerocephalus*, *Schoenus brevifoliusm*, *Xanthorrhoea resinosam Hakea teretifolia*, *Gleichenia dicarpa*	Banerjee et al., 2019
Bergen Hexa-copter, DJI Phantom 2, Phantom 3, & Mavic Pro, Nikon D800 DSLR & Tetracam MCA-6	Altitude = 10, 25m, Overlap = NL	5 m	Surface vegetation, EWM, Deeper areas of SAV, Water	*Myriophyllum spicatum* (Eurasian watermilfoil)	Brooks et al., 2019
DJI M600 Pro, Headwall Nano-Hyperspec imaging spectrometer, HyMap Sensor	Altitude = 115m, Overlap = 20%	5.1 – 5.4 cm	Unclassified, Bare ground, Emergent Vegetation (EMR), Water Hyacinth, Water Primrose, Riparian, Submerged Aquatic Vegetation, Water, Other Veg., Non-Photosynthetic Vegetation	Asphalt, Gravel, Bare soil, *Typha spp.*, *Phragmites australis*, *Arundo donax*, *Schoenoplectus spp.*, *Eichhornia crassipes*, *Ludwigia spp.*, Shrubs, Trees, *Salix app.*, *Egeria densa*, *Ceratophyllum demersum*, *Myriophyllum spicatum* *Hydrocotyle spp.*, *Azolla spp.*, Dead vegetation	Bolch et al., 2021
DJI Phantom 4 Pro, NL	Altitude = 86m, Overlap = NL	NL	Karst rivers and karst lakes, Karst herb, Water hyacinth, Construction land, Arable land, Lotus, Linden, Bamboo, Horse, Shadow	NL	Tang et al., 2019
DJI Phantom 4, RGB Camera	Altitude = 200m, Overlap = NL	< 10 cm	*S. alterniflora* patch	*Spartina alterniflora*	Zhu et al., 2019
SenseFly eBee+, Parrot Sequoia multispec. (1.2 MP)	Altitude = 148m, Overlap = NL	14.7 cm	Mesophilic, Meso-hygrophilic, Mesotrophic grassland, Hygrophilic, *Urtica dioica*, Bare soil and Water	*Lolium perenne*, *Poa trivialis* and *Ranunculus repens*, *Alopecurus geniculatus* and *Poa trivialis*, *Eleocharis acicularis* and *Agrostis stolonifera*, *Glyceria fluitans*	Alvarez-Vanhard et al., 2020
DJI M600, DJI Phantom 4, RIEGL VUX01UAV (LiDAR), RGB camera (1' CMOS, 12 MP)	Altitude = 100m (LiDAR), 200m Overlap = NL (LiDAR), 80% Forward) and 60% (Sidelap)	~ 8 cm	KO, AM, AC, SA, Mud flat, Water body	*Kandelia obovate*, *Avicennia marina*, *Aegiceras coniculatum*, *Spartina alterniflora*	Zhu et al., 2019

4.1 Accuracy acquisition challenges

All ground surveying is prone to multiple types of error (e.g., observer error or human biases, misidentification and counting errors; Elphick, 2008; Morrison, 2016) and accurate observation and recording are a function of field-measurement protocols and in-situ decisions. When field measurements were compared to those from the air (60 m above-ground level and with the sensors described previously) a loss of information was incurred due to the image resolution and the ability of data collected at that altitude to be used to detect the fine detail present at the ground level. Instances arose where visual observation of the imagery did not match ground observations, resulting in misclassification. However, automated classification, using a Random Tree classifier, was effective and when assessed against manual interpretation of image data collected the accuracy assessment was stronger than the comparison against in-situ measurements.

The comparison of classified remotely piloted aircraft acquired data against in-situ measurements was inhibited by several issues: sample size, a transdisciplinary approach, identification of plot locations, and image resolution (Figure **3**). Vegetation community

identification and classification was challenged for some classes where there was a small sample size. For example, it was difficult to differentiate Litter from Moss and Mixed Vegetation classes. While the field measurements provide a sample that was used to train our Random Tree classifier, the number of ground-based samples that included litter was small (n = 12). The small sample size limited the ability to train and accurately classify litter. Similarly, the ground survey work did not include Snags or Trees. Furthermore, edge-effect distortions along the tree line and sun exposure (i.e., strong reflection of incident solar radiation) reduced the ability of litter to be delineated from bare soil and other features. The identification of litter was a novel effort as a review of 15 articles in Remote Sensing (journal) have not included litter as a class to be delineated using remote sensing approaches.

While the project involved collaboration between a field biology team and a geomatics team, the relationship was akin to a transdisciplinary approach. The geomatics team derived a sampling approach for wetland selection, that was handed off to, and modified by the biology team. The biology team derived transects and plots, conducted plot measurements, then handed those data off to the geomatics team. A member of the biology team did collaborate with the geomatics team, in the computer lab, to assist with image interpretation. However, in hindsight, a more holistic field data collection in stronger collaboration could have strengthened the results through the following steps: remote-sensing classifier (individual) working on each field plot with the biology team; when collecting GPS receiver location points of field plots, include the edges of plots or face all plots in a standard cardinal direction as well as have the biologist walk around with the geomatics specialist to log 50-100 point locations with in-field classifications as checkpoints for training and testing data; and ensure that plots are free from canopy obstructions or explicitly acknowledge and measure above ground canopy layers.

There is often a desire to harmonize ground and aerial data by collecting those data synchronously. However, experience has demonstrated that this ideal is typically infeasible. For example, the field crew must be out of the field of view of aircraft sensors, therefore they must go into the field and establish plots (and measure) with visible plot and flagging markers, leave the study area, then return after the aircraft data collection to collect field survey materials. Not only does this further increase the length of time in the field, but multiple entries and exits can also affect the system of study and data collection (Bolding 2018). The issue of

harmonization is somewhat mitigated when sites and plots are used for repeated measurements. This harmonization would decrease the loss of memory – personal first-hand accounts of each location's environment, and limit the loss of information transferring the ground data up multiple scales to the aerial level. If additional sensors (e.g., LiDAR, Hyperspectral, and/or Thermal) were to be deployed, their abilities would improve the accuracy and ability to automate classification of wetland vegetation communities.

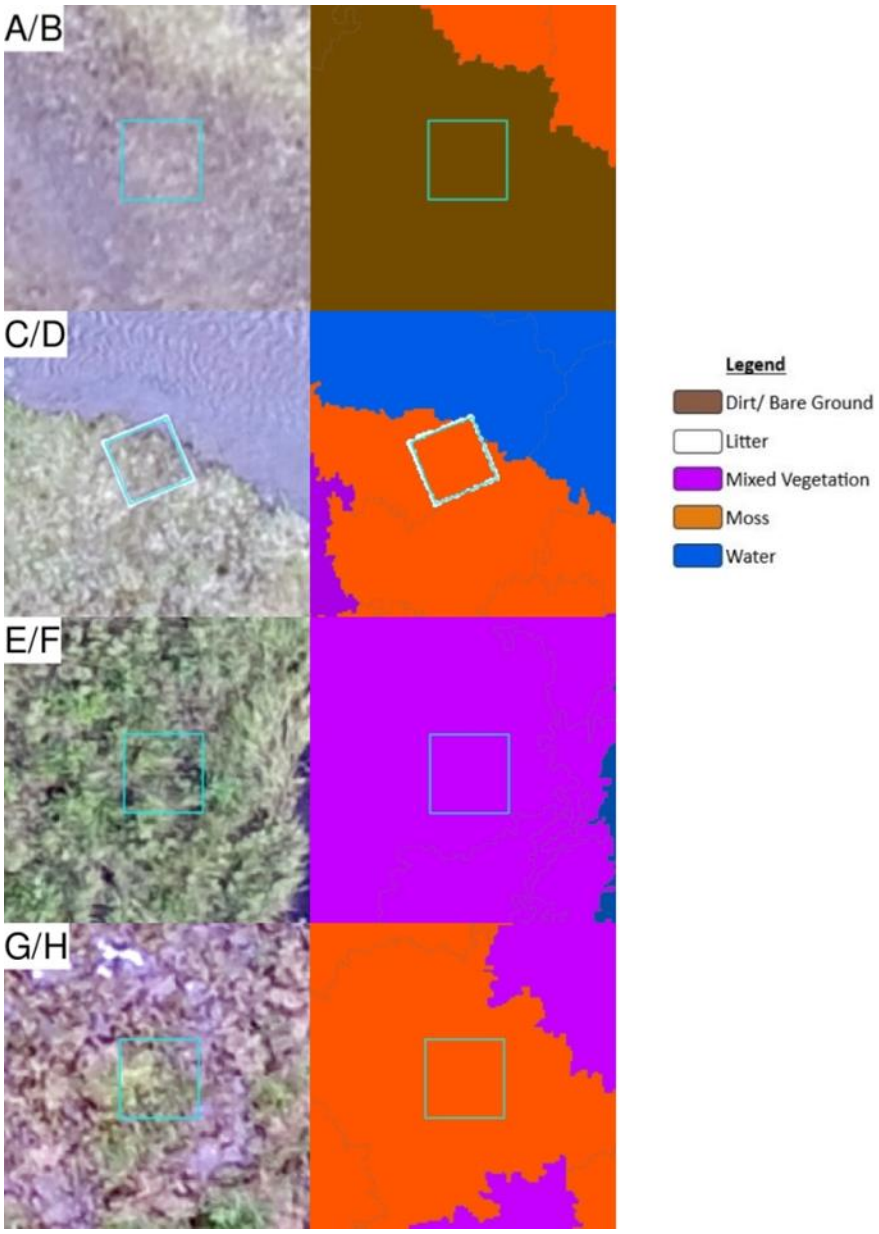


Figure 3: Standout misclassifications during comparison: litter classified as Dirt/bare ground (a/b), rock classified as moss (c/d), Litter classified as Mixed Veg (e/f) and water classified as moss (g/h). All images were captured at a scale of 1:25; Cyan blue square represents the field equipment (quadrat) used by the field team.

4.2 Future vegetation mapping with remotely piloted aircraft

The presented research utilized structure-from-motion multi-view stereo techniques with standard spectral wavelengths (i.e., red, green, blue, red-edge, and near-infrared). Sensors capable of acquiring data using other wavelengths (e.g., thermal, hyperspectral) as well as infrared- and green-wavelength light detection and ranging (LiDAR) sensors offer opportunities to improve upon the presented mapping and quantification of wetland vegetation communities. For example, infrared LiDAR can be used to penetrate the vegetation canopy (e.g., Reutebuch et al., 2003; Godone et al., 2018) to derive micro topography (e.g., Griffin et al., 2010; Nouwakpo et al., 2016) and canopy height, both of which can be used to improve vegetation classification (e.g., Gonzalez-Perez et al., 2022). Given that the most important image layer affecting the presented classification accuracy was the digital surface model (DSM; Section 3.1), it suggests that future efforts should incorporate LiDAR data to derive accurate vegetation height measurements. In lieu of those measurements, it should be possible to georeference structure-from-motion generated DSM heights from adjacent roadways or other hard surfaces to digital elevation/terrain models that would allow for the calculation of a true canopy height model. However, many of our study sites were distant from roadways or access roads were substantially higher than the wetland and were excluded from data acquisition to ensure aircraft safety. Furthermore, the lack of coordinated ground control points and differing resolutions among remotely piloted aircraft (e.g., 2.5 cm) collected elevation data and available DEMs (e.g., 10; Government of Alberta) could add substantial uncertainty to the derivation of a canopy height model between two datasets.

While the presented study was composed solely of peatland wetlands, the composition and configuration of vegetation around open-water, semi-permanent, and seasonal wetlands are a function of climate, topography, and land use (Daniel et al. 2022). Where water is present, green-wavelength LiDAR can be used to acquire bathymetry data (e.g., Tonina et al., 2018) that could be used to further inform and improve the classification of wetland vegetation communities. In addition to LiDAR sensors, improved classification and mapping of vegetation communities is possible through the use of hyper-spectral imaging, which has the potential to isolate specific and narrow wavelength bands (e.g., 10nm). Hyperspectral sensors have been used by multiple disciplines because of their ability to be deployed in space (i.e., satellites; Brando and Dekker, 2003; Gomez et al., 2008) as well as on on-board piloted and

remotely piloted aircraft (e.g., Bolch et al., 2021; Adão et al., 2017). When mounted on an RPA, hyperspectral sensors have been used to map chlorophyll content (e.g., Zhou et al., 2022), classify broad vegetation classes (Woody Vegetation and Herbaceous plants) (e.g., Samiappan et al., 2017) and specific plant communities (e.g., Phragmites australis, Typha orientalis, Suaeda glauca and Scirpus triqueter; Du et al., 2021). Their ability to derive spectral signatures for different types of vegetation suggests that the inclusion of hyperspectral data could improve the classification and mapping of the composition and configuration of wetland plant communities.

Lastly, thermal sensors have been used to monitor water temperature (e.g., Torgersen et al., 2001), aid in the detection of changes in wetland vegetation (e.g., Hwang et al., 2020), and have the potential to derive process measurements such as estimates of emissivity through repeated measurements. However, the temporally variability due to sun angles, cloud cover, and wind combined with the spatial variability at very fine resolutions (e.g., due to microtopography, neighbouring vegetation shading, and soil heterogeneity) have limited the use of thermal sensors to broader ecosystem measurements such as plant species diversity (Hamberg et al. 2020) and estimates of biological activity (e.g., Calderón et al., 2015). As in the presented research, use of the aforementioned sensors would require evaluation against in-situ measurements to understand the degree to which in-situ measurements and observations can be scaled to larger spatial extents through the use of remotely piloted aircraft.

Despite the current realized benefits and potential future benefits of the aforementioned sensors and RPAS applications, there is no set of standards in the literature to guide future research efforts on the sensor selection, sensor specifications, or flight characteristics (e.g., altitude above ground level, speed of flight, data overlap). For example, within the reviewed literature, flight altitudes ranged from 5m-200m, overlap ranged from 20% to 80%, and spatial resolutions varied resulting in final output resolutions between 1.4 cm and 14.7 cm (Table 6). In addition, many of the reviewed articles lacked information about the sensors, the flight characteristics, and data processing efforts that limit the utility of those efforts for others to build upon or replicate. There is a need for a standard set of reporting variables as well as a systematic assessment of how those reporting variables affect the accurate detection, identification, or classification of features of interest. To date, only Meinen and Robinson

(2020) have provided such a systematic assessment although their focus was on the contributions of different angles of image acquisition and number of ground control points on reconstructing terrain surfaces. A similar effort is immediately needed within the field of wetland ecology and remote sensing.

5.0 Conclusions

The importance of wetlands for the provision of habitat and biodiversity (e.g., Erwin, 2009), flood mitigation and improved water quality (e.g., Watson et al., 2016; Haberl et al., 2003), among many other services is well documented (e.g., Keddy, 2010). However, quantification of the composition and configuration of wetland vegetation communities remains sparse and yet is pivotal to many wetland functions and their ability to provide ecosystem services to society (e.g., Jiang et al., 2015). Recent developments in remotely piloted aircraft, and the myriad of sensors which they are able to deploy, has enabled the acquisition of very-high resolution data that can be used to improve our understanding of the composition and configuration of wetland vegetation. The presented research contributes to this point of intersection between ecology and remote sensing through the acquisition and analysis of optical and multispectral data at very-high spatial resolutions, 2.5 and 6.5 cm respectively, to 1) assess the accuracy of these data through automated classification (using random forests; 91% overall accuracy) as well as against in-situ plot measurements (55% overall accuracy); 2) improve our understanding of the importance of different spectral bands, vegetation indices, and remote sensing derivatives on classification accuracy, which were dominated by the digital surface model, followed by spectral bands and indices; and 3) summarize the composition and configuration of vegetation communities in wetland areas, which found that with increasing elevation the landscape became more heterogeneous with smaller patches of each vegetation type increasingly mixed with other types of vegetation. These contributions are important as ecologists are increasingly incorporating remotely piloted aircraft data collection (1-15 cm) and high-resolution satellite data (e.g., Sentinel – 10 m, Drusch et al., 2012; Pleiades – 0.5 m, Stumpf et al., 2014; and Planet – 0.5 m, Planet Labs PBC, 2023) to scale out empirical fieldwork to larger spatial extents. The presented research aims to guide future research by demonstrating that classification accuracy of Genus (land cover) can be high using standard remote-sensing training and testing data. However, high correspondence

to in-situ plot data (species level) require < 2 cm resolution data and a strong representation of plant structure captured by high-density LiDAR data. These findings are specific to high altitude peatlands that are void from the Canadian Wetland Classification System national data available in Canada and therefore should be assessed by others to see if similar findings are present at lower altitudes.

Chapter 3: Wetlands and wetland mapping in Canada

In 1973, The National Committee on Forest Lands set out to complete a national wetland classification in Canada (NWWG, 1997). Researchers began organizing and recording wetlands within Canada using a basic four-level system. Currently, within Canada, wetlands are classified using the Canadian Wetland Classification System (CWCS; National Wetlands Working group, 1997). Its first iteration was released in 1987 by the National Wetland Working Group and further refined to a second edition in 1997 (NWWG, 1997). To date, the classification system is based off a hierarchy that identifies a wetland's: (1) class, (2) form, and (3) type. In total, there are five different wetlands classes, differentiated by their formation (i.e., developmental characteristics) and environmental conditions. The five wetland classes are bogs, fens, marshes, swamps, and shallow waters. A wetlands form is reliant on environmental features that include its terrestrial surface, water features and the underlying soil composition. Lastly, the wetlands type is based off the vegetation communities associated within them (NWWG, 1997).

At the Federal level, wetland mapping is completed by Environment and Climate Change Canada (ECCC) (ECCC, 2016). The Government of Canada recently created a review titled "Canadian Environmental Sustainability Indicators: Extent of Canada's Wetlands (2016)". The goal aimed to measure the current extent of wetlands across the country and create a starting point for which future environmental changes can be measured. The projects intention is to inform proper management and handling of wetlands in Canada. Due to the absence of a national wetland monitoring system, the federal government has had to utilize data from multiple different sources such as Provincial Governments (e.g., Government of Newfoundland, British Columbia Ministry of Environment and Ontario Ministry of Natural Resources) and organizations (e.g., Ducks Unlimited). The data predominately used consists of remote sensing imagery, with wetlands then further mapped as vectors (e.g., shapefiles). Using the Canadian Wetland Classification System (CWCS) wetlands are further classified off the five main classes (i.e., bog, fen, marsh, swamp, and shallow water). If a wetland was unable to be classified off the five classes, they were labeled as "partially classified". Difficulties were inherent throughout the project due to the difference of vegetation amongst

wetland types and their seasonal variability. Also, ground surveys were required to limit the amount of error because the airborne imagery (e.g., satellites and aerial photographs) presented further classification issues due to inconsistent vegetation patterns. Overall, across the country accuracies vary regionally with northern areas presenting the most uncertainty because the extent of wetlands is often underestimated.

Within the Province of Alberta, where the 18 wetlands for this study reside, wetlands are classified using the Alberta Wetland Classification System (AWCS). The AWCS is a modified version of the existing CWCS to redefine a system specifically for the Province of Alberta (GOA, 2015). Within this classification system, wetlands are first divided into two main groups: Peatlands and Mineral wetlands. Peatlands consist of bogs and fens. Mineral wetlands consist of marshes, fens, and shallow open water. Wetlands are then further subdivided on the duration of inundated periods. The Alberta Government has also implemented a guideline to map and inventory wetlands across the province. Titled “Alberta Wetland Mapping: Standard and Guideline” (2020) the goal is to formalize a standard mapping process at the provincial scale with focus on the Prairie/Parkland and Boreal/Foothill zones located within Alberta. It intends to improve data quality for researchers and organizations conducting wetland mapping within the province (GOA,2020).

Other non-governmental organizations are also conducting wetland mapping within Canada. Ducks unlimited have been leaders in wetland mapping within Canada since 1979 (Ducks Unlimited, 2023). Using remote sensing imagery (e.g., aerial and satellite) Ducks Unlimited has mapped wetlands across Canada with estimates of millions of acres already completed (Ducks Unlimited, 2023). With the mapping currently completed, in 2002 Ducks Unlimited has created a database called “Canadian Wetland Inventory”, its interactive map can be viewed by the general public and researchers alike (https://maps.ducks.ca/cwi/). Conservation and restoration groups such as Nature Conservancy Canada (NCC) also conduct wetland mapping in Canada. Nature Conservancy Canada is a non-profit charity that utilizes a combination of different techniques to provide information for restoration. Their focus is protecting natural areas which include wetlands. Using remotely sensed data, ground surveys and historical data wetland mapping is completed to help visualize what vegetation communities are required to restore an area near or close to its original state (NCC, 2023)

The high-altitude wetlands studied in my thesis had not been previously mapped due to their isolated locations. The 18 wetlands observed were situated in remote areas, and accessibility was difficult at times with some requiring off-road vehicles or hiking required for access. Off-road vehicles were able to traverse logging roads that are not permanent roadways and are often of poor quality. There is a high probability that additional wetlands are present and remain unidentified in the areas surrounding the 18 observed wetlands, but accessibility is difficult with vehicles or a long a distance hiking on foot with equipment. This makes any potential opportunity expensive to fund a field team and highly time-consuming. Due to these constraints and challenges, RPAS becomes a viable solution for capturing the spatial scale required to quantify a whole wetland with fine resolution. RPAS provide the ability to capture extensive areas of land in a timely manner; multiple flights with an average 20-minute flight duration.

To determine what other inventory accuracies for peatland mapping in Canada have been done by researchers within academia I conducted a literature review across the Scopus database using the phrase (“Peatland” AND “Mapping” AND “Canada”). The search identified 40 possible articles of interest and further refinement was performed based off relevancy. Articles were considered relevant if they were conducted in Canada, a type of peatland, used remote sensing data, and mentioned overall accuracy. Additionally, if producer’s and user’s accuracy was available that was considered important and included. Of the 40 documents identified and reviewed (Table #), 10 documents met the minimum requirements and contained overall accuracies ranging from 31.7% to 93%. Two of the reviewed documents did not list producer’s and user’s accuracies; the article that did had a producer’s accuracy range of 11.8% to 100% and user’s accuracy range of 1.6% to 100%. None of the observed articles contained the same classes or total number of classes conducted within my thesis. There were a couple similar classes observed but overall, the reviewed articles mapped peatland/non peatland, peatland types (e.g., bogs or fens) or vegetation species commonly identified within peatlands.

Table 8: Inventory accuracies for peatland mapping in Canada. Observes overall accuracy (OA), producer's accuracy (PA) and user's accuracy (UA). NL = Not Listed

Accuracy Results			Authors
Overall Accuracy (OA)	Producer's Accuracy (PA)	User's Accuracy (UA)	
93%	81 to 100%	84 to 100%	Bourgeau et al., 2016
45.3 to 81.2%	NL	NL	Millard et al., 2020
81 to 84%	61.4 to100%	NL	Merchant et al., 2017
71.4%	NL	NL	Thompson et al., 2016
31.7 to 72.8%	11.8 to 83.5%	1.6 to 91.6%	Millard and Richardson, 2013
91.12%	77 to 96%	80 to 100%	Mahdianpari et al., 2021
84.7%	78.7 to 100%	60 to 100%	Grenier et al., 2008
86.6%	60.7%	69.5%	DeLancey et al., 2019
92%	84 to 100%	84 to96%	Granger et al., 2021
93%	86 to 96%	87 to 98%	Dribault et al., 2012

Initial observation of the random tree classifier against training sites obtained a high overall average (91%). With comparison to Table **8**, the 10 articles identified had overall accuracy range from 45.3 to 93%, which situates the classification results described in Chapter 2 at the upper end of 10-article accuracies. Similarly, the more specific producer's and user's accuracies from Chapter 2 were as good, if not better than the results observed in Table **8**. I obtained an overall producer's accuracy average of 87%, with a range of 63 to 98% and an overall user's accuracy average of 93%, with a range of 81 to 98%. None of the articles observed in Table **8** performed a comparison against in-situ plot measurements in a similar manner to what was done in Chapter 2. One article did perform ground truthing in the field, but field sites were classified by wetland type bog, fen, marsh, swamp or water (Mahdianpari, 2021) rather than wetland vegetation communities. When comparing my classification results against the in-situ measurements the overall accuracy decreased substantially to 54%. Though the results were not desirable, they are quite significant as no other article conducted a similar assessment to compare against. Articles that did perform some type of validation against their classifier extracted their validation points from airphotos where wetland type (e.g., Bog, fen, swamp, fen and water) through visual identification. Overall, the results I achieved provide valuable insights into how well the random tree classifier used in my study was able to effectively map wetland vegetation types.

Canadian wetlands are at risk of destruction from urban sprawl, agriculture, and resource extraction. As well, wetlands face an extreme risk to the ever-changing effects of climate change. Current improvements in remote sensing technologies have provided the ability to map wetlands in a more efficient manner, capable of capturing large areas of land with high resolution. Challenges are still present due to the high cost and time required for manual fieldwork. The remoteness of some wetlands also pose accessibility issues. The relevancy of my thesis to wetland mapping in Canada is its contribution in addressing the ongoing gaps in wetland mapping, the capabilities of deploying innovative technologies and provides insights on vegetation patterns within high-altitude wetlands. Overall, the contributions from my thesis highlight that high classification accuracy is achievable with Object Based Image Analysis (OBIA) using a random tree classifier (91% Overall Accuracy) as well with comparison against in-situ plot measurements (56% Overall Accuracy). I quantified how much weight each classification input (i.e., image bands, indices and DSM) contributed to the classification with the digital surface model (DSM) providing the highest influence and identified vegetation composition and configuration patterns that were influenced across increasing elevations. Overall, these results can provide a better understanding of these ecosystems and provide valuable information to aid future conservation or restoration efforts. In addition to the importance of these wetlands, my research highlights the need for a more collaborative and interdisciplinary approach to improve future wetland mapping within Canada.

References

Abeysinghe T, Milas AS, Arend K, Hohman B, Reil P, Gregory A, Vázquez-Ortega A (2019) Mapping Invasive Phragmites australis in the Old Woman Creek Estuary Using UAV Remote Sensing and Machine Learning Classifiers. Remote Sens. 11(11):1380. https://doi.org/10.3390/rs11111380

Adams DA, Buford MA, Dumond DM (1987) In search of the wetland boundary. Wetlands 7:59-70. https://doi.org/10.1007/BF03160803

Adão T, Hruška J, Pádua L, Bessa J, Peres E, Morais R, Sousa JJ (2017) Hyperspectral Imaging: A Review on UAV-Based Sensors, Data Processing and Applications for Agriculture and Forestry. Remote Sens. 9(11):1110. https://doi.org/10.3390/rs9111110

Albedo Space (2022) Certainty: Technical Specifications. Albedo Space Corporation. https://albedo.com/#certainty . Accessed 01 September 2023.

Alberta Environment and Sustainable Resource Development (ESRD) (2015) Alberta Wetland Classification System. Water Policy Branch, Policy and Planning Division, Edmonton, AB. https://open.alberta.ca/dataset/92fbfbf5-62e1-49c7-aa13-8970a099f97d/resource/1e4372ca-b99c-4990-b4f5-dbac23424e3a/download/2015-alberta-wetland-classification-system-june-01-2015.pdf. Accessed on 01 September 2023

Allende LK, Fletcher DT, Sun G (2011) Enhancing the removal of arsenic, boron and heavy metals in subsurface flow constructed wetlands using different supporting media. Water Sci Technol. 63(11):2612-2618. https://doi.org/10.2166/wst.2011.533

Alvarez-Vanhard E, Houet T, Mony C, Lecoq L, Corpetti T (2020) Can UAVs fill the gap between in situ surveys and satellites for habitat mapping? Remote Sens. Environ. 243 https://doi.org/10.1016/j.rse.2020.111780

Amani M, Salehi B, Mahdavi S, Granger JE, Brisco B, Hanson H (2017) Wetland Classification Using Multi-Source and Multi-Temporal Optical Remote Sensing Data in Newfoundland and Labrador, Canada. Can. J. Remote Sens. 43(7):360-373. https://doi.org/10.1080/07038992.2017.1346468

Ancin-Murguzur FJ, Munoz L, Monz C, Hausner VH (2020) Drones as a tool to monitor human impacts and vegetation changes in parks and protected areas. Remote Sens. Ecol. Conserv. 6(1):105-113. https://doi.org/10.1002/rse2.127

Anderson K, Bennie JJ, Milton EJ, Hughes PDM, Lindsay R, Meade R (2010). Combining LiDAR and IKONOS Data for Eco-Hydrological Classification of an Ombrotrophic Peatland. J. Environ. Qual. 39:260–273. https://doi.org/10.2134/jeq2009.0093

Baker C, Lawrence RL, Montagne C, Patten D (2007) Change detection of wetland ecosystems using Landsat imagery and change vector analysis. Wetlands 27:610-619. https://doi.org/10.1672/0277-5212(2007)27[610:CDOWEU]2.0.CO;2

Banerjee BP, Raval S, Cullen PJ, Singh SK (2019) Mapping of Complex Vegetation Communities and Species Using UAV-LIDAR Metrics and High-Resolution Optical Data. IGARSS 2019 – 2019 IEEE International Geoscience and Remote Sensing Symposium. 6110-6113. https://doi.org/10.1109/IGARSS.2019.8899160

Bertacchi A, Giannini V, Di Franco C, Silvestri N (2019) Using unmanned aerial vehicles for vegetation mapping and identification of botanical species in wetlands. Landscape Ecol. Eng. 15: 231–240. https://doi.org/10.1007/s11355-018-00368-1

Beyer F, Jurasinski G, Couwenberg J, Grenzdörffer G (2019) Multisensor data to derive peatland vegetation communities using a fixed-wing unmanned aerial vehicle. Int. J. Remote Sens. 40(24):9103-9125. https://doi.org/10.1080/01431161.2019.1580825

Bhantnagar S, Gill L, Ghosh B (2020) Drone Image Segmentation Using Machine and Deep Learning for Mapping Raised Bog Vegetation Communities. Remote Sens. 12(16):2602. https://doi.org/10.3390/rs12162602

Bolch EA, Hestir EL, Khanna S (2021) Performance and Feasibility of Drone-Mounted Imaging Spectroscopy for Invasive Aquatic Vegetation Detection. Remote Sens. 13(4):582. https://doi.org/10.3390/rs13040582

Bolding M (2018) Vegetation Based Assessment of Wetland Condition in the Prairie Pothole Region. Dissertation, University of Waterloo. http://hdl.handle.net/10012/12921

Borchert SM, Osland MJ, Enwright NM, Griffith KT (2017) Coastal wetland adaptation to sea level rise: Quantifying potential for landward migration and coastal squeeze. J. Appl. Ecol. 55(6):2876-2887. https://doi.org/10.1111/1365-2664.13169

Bourgeau-Chavez LL, Endres S, Powell R, Battaglia MJ, Benscoter B, Turetsky M, Kasischke ES, Banda E (2016) Mapping boreal peatland ecosystem types from multitemporal radar and optical satellite imagery. Can. J. For. Res. 47(4):545-559. https://doi.org/10.1139/cjfr-2016-0192

Bow River Basin Counsel (2021) BRBC Library. Government of Alberta. https://brbc.ab.ca/brbc-library. Accessed 01 September 2023

Brando VE, Dekker AG (2003) Satellite hyperspectral remote sensing for estimating estuarine and coastal water quality. IEEE Trans. Geosci. Remote Sens. 41(6): 1378-1387. https://doi.org/10.1109/TGRS.2003.812907

Breiman L (2001) Random Forests. Mach. Learn. 45:5-32. https://doi.org/10.1023/A:1010933404324

Brooks CN, Grimm AG, Marcarelli AM, Dobson RJ (2019) Multiscale collection and analysis of submerged aquatic vegetation spectral profiles for Eurasian watermilfoil detection. J. Appl. Remote Sens. 13(3):037501. https://doi.org/10.1117/1.JRS.13.037501

Broussard (III) WP, Visser JM, Brooks RP (2022) Quantifying Vegetation and Landscape Metrics with Hyperspatial Unmanned Aircraft System Imagery in a Coastal Oligohaline Marsh. Estuaries and Coasts 45:1058-1069. https://doi.org/10.1007/s12237-020-00828-8

Cabezas M, Kentsch S, Tomhave L, Gross J, Caceres MLL, Diez Y (2020) Detection of Invasive Species in Wetlands: Practical DL with Heavily Imbalanced Data. Remote Sens. 12(20):3431. https://doi.org/10.3390/rs12203431

Calderón R, Navas-Cortés JA, Zarco-Tejada PJ (2015) Early Detection and Quantification of Verticillium Wilt in Olive Using Hyperspectral and Thermal Imagery over Large Areas. Remote Sens. 7(5):5584-5610. https://doi.org/10.3390/rs70505584

Canisius F, Wang S, Croft H, Leblanc SG, Russell HAJ, Chen J, Wang R (2019) A UAV-Based Sensor System for Measuring Land Surface Albedo: Tested over a Boreal Peatland Ecosystem. Drones 3(1):27. https://doi.org/10.3390/drones3010027

Carney K, Sydeman W (1999) A Review of Human Disturbance Effects on Nesting Colonial Waterbirds. Waterbirds 22(1):68-79. https://doi.org/10.2307/1521995

Ciężkowski W, Szporak-Wasilewska S, Kleniewska M, Jóźwiak J, Gnatowski T, Dąbrowski P, Góraj M, Szatyłowicz J, Ignar S, Chormański J (2020) Remotely Sensed Land Surface Temperature-Based Water Stress Index for Wetland Habitats. Remote Sens. 12(4):631. https://doi.org/10.3390/rs12040631

Congalton RG (1991) A review of assessing the accuracy of classifications of remotely sensed data. Remote Sens. Environ. 37(1):35-46. https://doi.org/10.1016/0034-4257(91)90048-B

Dabrowska-Zielinska K, Budzynska M, Tomaszewska M, Malinkska A, Gatkowska M, Bartold M, Malek I (2016) Assessment of carbon flux and soil moisture in wetlands applying Sentinel-1 data. Remote Sens. 8(9):756-768. https://doi.org/10.3390/rs8090756

Dale J, Burnside NG, Hill-Butler C, Berg MJ, Strong CJ, Burgess HM (2020) The Use of Unmanned Aerial Vehicles to Determine Differences in Vegetation Cover: A Tool for Monitoring Coastal Wetland Restoration Schemes. Remote Sens. 12(24):4022. https://doi.org/10.3390/rs12244022

Daniel J, Rooney RC, Robinson DT (2022) Climate, land cover and topography: essential ingredients in predicting wetland permanence. Biogeosciences 19:1547-1570. https://doi.org/10.5194/bg-19-1547-2022

DeLancey ER, Kariyeva J, Bried JT, Hird JN (2019) Large-scale probabilistic identification of boreal peatlands using Google Earth Engine, open-access satellite data, and machine learning. PLOS ONE 14(6):e0218165. https://doi.org/10.1371/journal.pone.0218165

Dewan AM, Yamaguchi Y (2009) Land use and land cover change in Greater Dhaka, Bangladesh: Using remote sensing to promote sustainable urbanization. Appl. Geogr. 29(3):390-401. https://doi.org/10.1016/j.apgeog.2008.12.005

Díaz-Delgado R, Cazacu C, Adamescu M (2019) Rapid Assessment of Ecological Integrity for LTER Wetland Sites by Using UAV Multispectral Mapping. Drones 3(1):3. https://doi.org/10.3390/drones3010003

Doughty CL, Cavanaugh KC (2019) Mapping Coastal Wetland Biomass from High Resolution Unmanned Aerial Vehicle (UAV) Imagery. Remote Sens. 11(5):540. https://doi.org/10.3390/rs11050540

Dribault Y, Chokmani K, Bernier M (2012) Monitoring Seasonal Hydrological Dynamics of Minerotrophic Peatlands Using Multi-Date GeoEye-1 Very High Resolution Imagery and Object-Based Classification. Remote Sens. 4(7): 1887-1912. https://doi.org/10.3390/rs4071887

Drusch M, Del Bello U, Carlier S, Colin O, Fernandez V, Gascon F, Hoersch B, Isola C, Laberinti P, Martimort P, Maygret A, Spoto F, Sy O, Marchese F, Bargellini (2012) Sentinel-2: ESA's Optical High-Resolution Mission for GMES Operational Services. Remote Sens. Environ. 15:25-36. https://doi.org/10.1016/j.rse.2011.11.026

Ducks Unlimited (2023) Wetlands. Ducks Unlimited Canada. https://www.ducks.ca/our-work/wetlands/what-is-a-wetland/. Accessed 17 October 2023

Du B, Mao D, Wang Z, Qiu Z, Yan H, Feng K, Zhang Z (2021) Mapping Wetland Plant Communities Using Unmanned Aerial Vehicle Hyperspectral Imagery by Comparing Object/Pixel-Based Classifications Combining Multiple Machine-Learning Algorithms. IEEE J. Sel. Top. Appl. Earth Obs. Remote Sens. 14:8249-8258. https://doi.org/10.1109/JSTARS.2021.3100923

Elphick CS (2008) How you count counts: the importance of methods research in applied ecology. J. Appl. Ecol. 45(5):1313-1320. https://doi.org/10.1111/j.1365-2664.2008.01545.x

Erwin KL (2009) Wetlands and global climate change: the role of wetland restoration in a changing world. Wetlands Ecol. Manage. 17:71-84. https://doi.org/10.1007/s11273-008-9119-1

ESRI 2011. ArcGIS Desktop: Release 10. Redlands, CA: Environmental Systems Research Institute

ESRI (2023) Buffer (Analysis). ESRI. https://pro.arcgis.com/en/pro-app/latest/tool-reference/analysis/buffer.htm#L_. Accessed 01 September 2023

ESRI (2023) Feature Envelope To Polygon (Data Management). ESRI. https://pro.arcgis.com/en/pro-app/latest/tool-reference/data-management/feature-envelope-to-polygon.htm. Accessed 01 September 2023

ESRI (2023) Watershed (Spatial Analyst). ESRI. https://pro.arcgis.com/en/pro-app/3.0/tool-reference/spatial-analyst/watershed.htm . Accessed 13 October 2023

ESRI (2023) What is GIS? ESRI https://www.esri.com/en-us/what-is-gis/overview. Accessed 15 October 2023

Evans I, Robinson DT, Rooney RC (2017) A methodology for relating wetland configuration to human disturbance in Alberta. Landscape Ecol. 32:2059-2076. https://doi.org/10.1007/s10980-017-0566-z

Fang C, Tao Z, Gao D, Wu H (2016) Wetland mapping and wetland temporal dynamic analysis in the Nanjishan wetland using Gaofen One data. Ann. Gis 22(4):259-271. https://doi.org/10.1080/19475683.2016.1231719

Feagin RA, Johns N, Huff TP, Abdullah MM, Fritz-Grammond K (2020) Restoration of Freshwater Inflows: the Use of Spatial Analysis for Hydrologic Planning in the Anahuac National Wildlife Refuge, USA. Wetlands 40:2561-2576. https://doi.org/10.1007/s13157-020-01318-0

Fickas KC, Cohen WB, Yang Z (2016) Landsat-based monitoring of annual wetland change in the Willamette Valley of Oregon, USA from 1972-2012. Wetlands Ecol. Manage. 24:73-92. https://doi.org/10.1007/s11273-015-9452-0

Flores-de-Santiago F, Valderrama-Landeros L, Rodríguez-Sobreyra R, Flores-Verdugo F (2020) Assessing the effect of flight altitude and overlap on orthoimage generation for UAV estimates of coastal wetlands. J. Coastal Conserv. 4(35). https://doi.org/10.1007/s11852-020-00753-9

Francis RJ, Lyons MB, Kingsford RT, Brandis KJ (2020) Counting Mixed Breeding Aggregations of Animal Species Using Drones: Lessons from Waterbirds on Semi-Automation. Remote Sens. 12(7):1185. https://doi.org/10.3390/rs12071185

Fuller LM, Morgan TR, Aichele SS (2006). Wetland delineation with IKONOS high-resolution satellite imagery, Fort Custer Training Center, Battle Creek, Michigan, 2005 (No. 2006-5051). US Geological Survey. https://doi.org/10.3133/sir20065051

Furlan LM, Moreira CA, Guilherme de Alencar P, Rosolen V (2021) Environmental monitoring and hydrological simulations of a natural wetland based on high-resolution unmanned aerial vehicle data (Paulista Peripheral Depression, Brazil). Environ. Challenges 4:100146. https://doi.org/10.1016/j.envc.2021.100146

Gagnon P, Coleman DJ (1990) Geomatics an integrated, systemic approach to meet the needs for spatial information. Canadian Institute of Surveying and Mapping Journal. 44(4): 377-382. https://doi.org/10.1139/geomat-1990-0033

Gandarillas VR, Jiang Y, Irvine K (2016) Assessing the services of high mountain wetlands in tropical Andes: A case study of Caripe wetlands at Bolivian Altiplano. Ecosyst. Serv. 19:51-64. https://doi.org/10.1016/j.ecoser.2016.04.006

Geng R, Jin S, Fu B, Wang B (2020) Object-Based Wetland Classification Using Multi-Feature Combination of Ultra-High Spatial Resolution Multispectral Images. Can. J. Remote Sens. 46(6):784-802. https://doi.org/10.1080/07038992.2021.1872374

Gleason RA, Tangen BA, Browne BA, Euliss NH Jr (2009) Greenhouse gas flux from cropland and restored wetlands in the Prairie Pothole Region. Soil Biol. Biochem. 41(12):2501-2507. https://doi.org/10.1016/j.soilbio.2009.09.008

Godone D, Giordan D, Baldo M (2018) Rapid mapping application of vegetated terraces based on high resolution airborne LiDAR. Geomatics Nat. Hazards Risk 9(1):970-985. https://doi.org/10.1080/19475705.2018.1478893

Gomarasca MA (2010) Basics of geomatics. Appl Geomat. 2:137–146. https://doi.org/10.1007/s12518-010-0029-6

Gomez C, Rossel RAR, McBratney AB (2008) Soil organic carbon prediction by hyperspectral remote sensing and field vis-NIR spectroscopy: An Australian case study. Geoderma 146(3-4):403-411. https://doi.org/10.1016/j.geoderma.2008.06.011

Gonzalez-Perez A, Abd-Elrahman A, Wilkinson B, Johnson DJ, Carthy RR (2022) Deep and Machine Learning Image Classification of Coastal Wetlands Using Unpiloted Aircraft System Multispectral Images and Lidar Datasets. Remote Sens. 14(16):3937. https://doi.org/10.3390/rs14163937

Granger JE, Mahdianpari M, Puestow T, Warren S, Mohammadimanesh F, Salehi B, Brisco B (2021) Object-based random forest wetland mapping in Conne River, Newfoundland, Canada. J. Appl. Remote Sens. 15(3):038506. https://doi.org/10.1117/1.JRS.15.038506

Grenier M, Labrecque S, Garneau M, Tremblay A (2008) Object-based classification of a SPOT-4 image for mapping wetlands in the context of greenhouse gases emissions: the case of the Eastmain region, Québec, Canada. Can. J. Remote Sens. 34(2):398-413. https://doi.org/10.5589/m08-049

Griffin LF, Knight JM, Dale PER (2010) Identifying Mosquito Habitat Microtopography in an Australian Mangrove Forest Using LiDAR Derived Elevation Data. Wetlands 30:929-937. https://doi.org/10.1007/s13157-010-0089-8

Gustafson EJ (1998) Quantifying Landscape Spatial Pattern: What Is the State of the Art? Ecosystems 1:143-156. https://doi.org/10.1007/s100219900011

Hamberg JL, Fraser RA, Robinson DT, Trant AJ, Murphy SD (2020) Surface temperature as an indicator of plant species diversity and restoration in oak woodland. Ecol. Indic. 113:106249. https://doi.org/10.1016/j.ecolind.2020.106249

Haberl R, Grego S, Langergraber G, Kadlec RH, Cicalini AR, Dias SM, Novais JM, Aubert S, Gerth A, Thomas H, Hebner A (2003) Constructed wetlands for the treatment of organic pollutants. J. Soils Sediments 3:109-124. https://doi.org/10.1007/BF02991077

Harvey MC, Hare DK, Hackman A, Davenport G, Haynes AB, Helton A, Lane JW Jr., Briggs MA (2019) Evaluation of Stream and Wetland Restoration Using UAS-Based Thermal Infrared Mapping. Water 11(8):1568. https://doi.org/10.3390/w11081568

He L, Li A, Yin G, Nan X, Bian J (2019) Retrieval of grassland aboveground biomass through inversion of the PROSAIL model with MODIS imagery. Remote Sens.11(13):1597. https://doi.org/10.3390/rs11131597

Helm C, Hassan MA, Reid D (2020) Characterization of morphological units in a small, forested stream using close-range remotely piloted aircraft imagery. Earth Surf. Dyn. 8(4): 913-929. https://doi.org/doi:10.5194/esurf-8-913-2020

Hernández-Romero G, Álvarez-Martínez JM, Pérez-Silos I, Silió-Calzada A, Vieites DR, Barquín J (2022) From Forest Dynamics to Wetland Siltation in Mountainous Landscapes: A RS-Based Framework for Enhancing Erosion Control. Remote Sens. 14(8):1864. https://doi.org/10.3390/rs14081864

Hladik C, Alber M (2012) Accuracy assessment and correction of a LiDAR-derived salt marsh digital elevation model. Remote Sens. Environ. 121:224-235. https://doi.org/10.1016/j.rse.2012.01.018

Holden PB, Rebelo AJ, New MG (2021) Mapping invasive alien trees in water towers: A combined approach using satellite data fusion, drone technology and expert engagement. Remote Sens. Appl.: Soc. Environ. 21: 100448. https://doi.org/10.1016/j.rsase.2020.100448

Huang C, Peng Y, Lang M, Yeo IY, McCarty G (2014) Wetland inundation mapping and change monitoring using Landsat and airborne LiDAR data. Remote Sens. Environ. 141:231-242. https://doi.org/10.1016/j.rse.2013.10.020

Hwang K, Chandler DG, Shaw SB (2020) Patch scale evapotranspiration of wetland plant species by ground-based infrared thermometry. Agric. For. Meteorol. 287:107948. https://doi.org/10.1016/j.agrformet.2020.107948

Iljas T (2022) Using Very High Resolution Remotely Piloted Aircraft Imagery to Map Peatland Vegetation Composition and Configuration Patterns within an Elevation Gradient. Dissertation, University of Waterloo. http://hdl.handle.net/10012/18006

Immitzer M, Atzberger C, Koukal T (2012) Tree Species Classification with Random Forest Using Very High Spatial Resolution 8-Band WorldView-2 Satellite Data. Remote Sens. 4(9):2661-2693. https://doi.org/10.3390/rs4092661

Jeziorska J (2019) UAS for Wetland Mapping and Hydrological Modeling. Remote Sens. 11(17):1997. https://doi.org/10.3390/rs11171997

Jiang L, Bandini F, Smith O, Jensen IK, Bauer-Gottwein P (2020) The Value of Distributed High-Resolution UAV-Borne Observations of Water Surface Elevation for River Management and Hydrodynamic Modeling. Remote Sens. 12(7):1171. https://doi.org/10.3390/rs12071171

Jiang B, Wong CP, Chen Y, Cui L, Ouyang Z (2015) Advancing Wetland Policies Using Ecosystem Services – China's Way Out. Wetlands 35(5):983-995. https://doi.org/10.1007/s13157-015-0687-6

Ju Y, Bohrer G (2022) Classification of Wetland Vegetation Based on NDVI Time Series from the HLS Dataset. Remote Sens. 14(9), 2107. https://doi.org/10.3390/rs14092107

Kalacska M, Arroyo-Mora JP, de Gea J, Snirer E, Herzog C, Moore TR (2013) Videographic Analysis of Eriophorum Vaginatum Spatial Coverage in an Ombotrophic Bog. Remote Sens. 5(12):6501-6512. https://doi.org/10.3390/rs5126501

Kalacska M, Chmura GL, Lucanus O, Bérubé D, Arroyo-Mora JP (2017) Structure from motion will revolutionize analyses of tidal wetland landscapes. Remote Sens. Environ. 199:14-24. https://doi.org/10.1016/j.rse.2017.06.023

Kaplan G, Avdan U (2018) Monthly Analysis of Wetlands Dynamics Using Remote Sensing Data. ISPRS Int. J. Geo-Inf. 7(10):411. https://doi.org/10.3390/ijgi7100411

Keddy P (2010) Services and function. In Wetland Ecology: Principles and Conservation. Cambridge: Cambridge University Press, pp. 300-329. https://doi.org/10.1017/CBO9780511778179.013

Kelly M, Tuxen KA, Stralberg D (2011) Mapping changes to vegetation pattern in a restoring wetland: Finding pattern metrics that are consistent across spatial scale and time. Ecol. Indic. 11(2):263-273. https://doi.org/10.1016/j.ecolind.2010.05.003

Kentsch S, Cabezas M, Tomhave L, Groß J, Burkhard B, Caceres MLL, Waki K, Diez Y (2021) Analysis of UAV-Acquired Wetland Orthomosaics Using GIS, Computer Vision, Computational Topology and Deep Learning. Sensors 21(2):471. https://doi.org/10.3390/s21020471

Kuhn M (2008). Caret package. Journal of Statistical Software, 28(5). https://CRAN.R-project.org/package=caret

Liu J, Chen J, Qin Q, You H, Han X, Zhou G (2020) Patch Pattern and Ecological Risk Assessment of Alpine Grassland in the Source Region of the Yellow River. Remote Sens. 12(20):3460. https://doi.org/10.3390/rs12203460

Liu T, Abd-Elrahman A (2018) Multi-view object-based classification of wetland land covers using unmanned aircraft system images. Remote Sens. Environ. 216:122-138. https://doi.org/10.1016/j.rse.2018.06.043

Liu J, Liu X, Wang Y, Li Y, Jiang Y, Fu Y, Wu J (2020) Landscape composition or configuration: which contributes more to catchment hydrological flows and variations? Landscape Ecol. 35:1531-1551. https://doi.org/10.1007/s10980-020-01035-3

Lorena AC, Jacintho LFO, Siqueira MF, De Giovanni R, Lohmann LG, de Carvalho ACPLF, Yamamoto M (2011) Comparing machine learning classifiers in potential distribution modelling. Expert Syst. Appl. 38(5):5268-5275. https://doi.org/10.1016/j.eswa.2010.10.031

Mahdianpari M, Granger JE, Mohammadimanesh F, Warren S, Puestow T, Salehi B, Brisco B (2021) Smart solutions for smart cities: Urban wetland mapping using very-high resolution satellite imagery and airborne LiDAR data in the City of St. John's, NL, Canada. J. Environ. Manage. 280:111676. https://doi.org/10.1016/j.jenvman.2020.111676

Marcaccio JV, Markle CE, Chow-Fraser P (2016) Use of fixed-wing and multi-rotor unmanned aerial vehicles to map dynamic changes in a freshwater marsh. Journal of Unmanned Vehicle Systems 4(3):193-202. https://doi.org/10.1139/juvs-2015-0016

Mather PM (1999) Computer Processing of Remotely-Sensed Images: An Introduction. Wiley, Chichester, UK. https://doi.org/10.1002/9780470666517

Maxa M, Bolstad P (2009) Mapping northern wetlands with high resolution satellite images and LiDAR. Wetlands. 29:248–260. https://doi.org/10.1672/08-91.1

McFeeters SK (1996) The use of the Normalized Difference Water Index (NDWI) in the delineation of open water features. Int. J. Remote Sens. 17(7):1425-1432. https://doi.org/10.1080/01431169608948714

Medvedev A, Telnova N, Alekseenko N, Koshkarev A, Kuznetchenko P, Asmaryan S, Narykov A (2020) UAV-Derived Data Application for Environmental Monitoring of the Coastal Area of Lake Sevan, Armenia with a Changing Water Level. Remote Sens. 12(22):3821. https://doi.org/10.3390/rs12223821

Meinen BU, Robinson DT (2020) Mapping erosion and deposition in an agricultural landscape: Optimization of UAV image acquisition schemes for SfM-MVS. Remote Sens. Environ. 239:111666. https://doi.org/10.1016/j.rse.2020.111666

Merchant MA, Adams JR, Berg AA, Baltzer JL, Quinton WL, Chasmer LE (2017) Contributions of C-Band SAR Data and Polarimetric Decompositions to Subarctic Boreal Peatland Mapping. IEEE J. Sel. Top. Appl. Earth Obs. Remote Sens. 10(4): 1467-1481. https://doi.org/10.1109/JSTARS.2016.2621043

Millard K, Kirby P, Nandlall S, Behnamian A, Banks S, Pacini F (2020) Using Growing-Season Time Series Coherence for Improved Peatland Mapping: Comparing the Contributions of Sentinel-1 and RADARSAT-2 Coherence in Full and Partial Time Series. Remote Sens. 12(15):2465. https://doi.org/10.3390/rs12152465

Millard K, Richardson M (2013) Wetland mapping with LiDAR derivatives, SAR polarimetric decompositions, and LiDARSAR fusion using a random forest classifier. Can. J. Remote Sens. 39(4):290-307. https://doi.org/10.5589/m13-038

Mitsch WJ, Bernal B, Nahlik AM, Mander Ü, Zhang L, Anderson CJ, Jørgensen SE, Brix H (2013) Wetlands, carbon, and climate change. Landscape Ecol. 28:583-597. https://doi.org/10.1007/s10980-012-9758-8

Mitsch WJ, Taylor JR, Benson KB, Hill PL (1983) Wetlands and coal surface mining in Western Kentucky — A regional impact assessment. Wetlands 3(1):161-179. https://doi.org/10.1007/BF03160739

Morrison LW (2016) Observer error in vegetation surveys: a review. J. Plant Ecol. 9(4):367-379. https://doi.org/10.1093/jpe/rtv077

Mui A, He Y, Weng Q (2015) An object-based approach to delineate wetlands across landscapes of varied disturbance with high spatial resolution satellite imagery. ISPRS J. Photogramm. Remote Sens. 109:30-46. https://doi.org/10.1016/j.isprsjprs.2015.08.005

Mueller N, Lewis A, Roberts D, Ring S, Melrose R, Sixsmith J, Lymburner L, McIntyre A, Tan P, Curnow S, Ip A (2016) Water observations from space: Mapping surface water from 25 years of Landsat imagery across Australia. Remote Sens. Environ. 174:341-352. https://doi.org/10.1016/j.rse.2015.11.003

Munoz B, Lesser VM, Dorney JR, Savage R (2009) A proposed methodology to determine accuracy of location and extent of geographically isolated wetlands. Environ. Monit. Assess. 150:53-64. https://doi.org/10.1007/s10661-008-0672-0

Mutanga O, Adam E, Cho MA (2012) High density biomass estimation for wetland vegetation using WorldView-2 imagery and random forest regression algorithm. Int. J. Appl. Earth Obs. Geoinf. 18:399-406. https://doi.org/10.1016/j.jag.2012.03.012

National Wetlands Working Group (1997) The Canadian Wetland Classification System. 2nd edition. Edited by BG Warner and CDA Rubec. Wetlands Research Centre, University of Waterloo, Waterloo, Ontario.

Natural Regions Committee (2006). Natural Regions and Subregions of Alberta. Compiled by D.J. Downing and W.W. Pettapiece. Government of Alberta. Pub. No. T/852. https://www.albertaparks.ca/media/2942026/nrsrcomplete_may_06.pdf Accessed 21 November 2022

NCC (2023) Ecosystem Restoration. Nature Conservancy of Canada. https://www.natureconservancy.ca/en/what-we-do/ecosystem-restoration/. Accessed 17 October 2023

Newport Corporation (2023) Light Detection and Ranging. Newport Corporation. https://www.newport.com/n/lidar. Accessed 16 October 2023

Nguyen C, Starek MJ, Tissot P, Gibeaut J (2019) Unsupervised Clustering of Multi-Perspective 3D Point Cloud Data in Marshes: A Case Study. Remote Sens. 11(22):2715. https://doi.org/10.3390/rs11222715

Nouwakpo SK, Weltz MA, McGwire K (2016) Assessing the performance of structure-from-motion photogrammetry and terrestrial LiDAR for reconstructing soil surface microtopography of naturally vegetated plots. Earth Surf. Processes Landforms 41(3):308-322. https://doi.org/10.1002/esp.3787

Oddi L, Cremonese E, Ascari L, Filippa G, Galvagno M, Serafino D, di Cella UM (2021) Using UAV Imagery to Detect and Map Woody Species Encroachment in a Subalpine Grassland: Advantages and Limits. Remote Sens. 13(7):1239. https://doi.org/10.3390/rs13071239

Olofsson P, Foody GM, Herold M, Stehman SV, Woodcock CE, Wulder AM (2014) Good practices for estimating area and assessing accuracy of land change. Remote Sens. Environ. 148:42-57. https://doi.org/10.1016/j.rse.2014.02.015

Pande-Chhetri R, Abd-Elrahman A, Liu T, Morton J, Wilhelm VL (2017) Object-based classification of wetland vegetation using very high-resolution unmanned air system imagery. Eur. J. Remote Sens. 50(1):564-576. https://doi.org/10.1080/22797254.2017.1373602

Park MH, Stenstrom MK (2008) Classifying environmentally significant urban land uses with satellite imagery. J. Environ. Manage. 86(1):181–192. https://doi.org/10.1016/j.jenvman.2006.12.010

Pashaei M, Kamangir H, Starek MJ, Tissot P (2020) Review and Evaluation of Deep Learning Architectures for Efficient Land Cover Mapping with UAS Hyper-Spatial Imagery: A Case Study Over a Wetland. Remote Sens. 12(6):959. https://doi.org/10.3390/rs12060959

Paudel D, Boogaard H, de Wit A, Janssen S, Osinga S, Pylianidis C, Athanasiadis IN (2021) Machine learning for large-scale crop yield forecasting. Agric. Syst. 187: 103016. https://doi.org/10.1016/j.agsy.2020.103016

Pérez-Ortiz M, Peña JM, Gutiérrez PA, Torres-Sánchez J, Hervás-Martínez C, López-Granados F (2015) A semi-supervised system for weed mapping in sunflower crops using unmanned aerial vehicles and a crop row detection method. Appl. Soft Comput. 37:533-544. https://doi.org/10.1016/j.asoc.2015.08.027

Petus C, Lewis M, White D (2013) Monitoring temporal dynamics of Great Artesian Basin wetland vegetation, Australia, using MODIS NDVI. Ecol. Indic. 247:829-839. https://doi.org/10.1016/j.jenvman.2019.06.098

Pinton D, Canestrelli A, Wilkinson B, Ifju P, Ortega A (2020) A new algorithm for estimating ground elevation and vegetation characteristics in coastal salt marshes from high-resolution UAV-based LiDAR point clouds. Earth Surf. Processes Landforms 45(14):3687-3701. https://doi.org/10.1002/esp.4992

Planet Labs PBC (2023) Planet Analytic Imagery And Archive. Planet Labs PBC. https://www.planet.com/products/planet-imagery/ .Accessed 01 September 2023

Prisley SP, Turner JA, Brown MJ, Schilling E, Lambert SG (2020) Uncertainty of Forested Wetland Maps Derived from Aerial Photography. Photogramm Eng Remote Sensing 86(10):609-617. https://doi.org/10.14358/PERS.86.10.609

Province of Alberta (2022) Public Lands Act, c P-40. Alberta King's Printer. https://kings-printer.alberta.ca/1266.cfm?page=P40.cfm&leg_type=Acts&isbncln=9780779824960.Accessed 01 September 2023

QGIS.org (2023). QGIS Geographic Information System. Open Source Geospatial Foundation Project. http://qgis.or

Raeva P, Pavelka K Jr (2020) Optimized Post-Processing of Multiple Uav Images for Forestry Inspections. ISPRS Ann. Photogramm. Remote Sens. Spatial Inf. Sci. XLIII-B1:15-19. https://doi.org/10.5194/isprs-archives-XLIII-B1-2020-15-2020

Rebelo LM, Finlayson CM, Nagabhatla N (2009) Remote sensing and GIS for wetland inventory, mapping and change analysis. J. Environ. Manage. 90(7):2144-2153. https://doi.org/10.1016/j.jenvman.2007.06.027

Reutebuch SE, McGaughey RJ, Anderson HE, Carson WW (2003) Accuracy of a high-resolution lidar terrain model under a conifer forest canopy. Can. J. Remote Sens. 29(5):527-535. https://doi.org/10.5589/m03-022

Rhee DS, Kim YD, Kang B, Kim D (2018) Applications of unmanned aerial vehicles in fluvial remote sensing: An overview of recent achievements. KSCE J. Civ. Eng. 22:588-602. https://doi.org/10.1007/s12205-017-1862-5

Ruiz-Jimenez J, Zanca N, Lan H, Jussila M, Hartonen K, Riekkola MJ (2019) Aerial drone as a carrier for miniaturized air sampling systems. J. Chromatogr. A 1597:202-208. https://doi.org/10.1016/j.chroma.2019.04.009

Samiappan S, Turnage G, Hathcock L, Yao H, Kincaid R, Moorhead R, Ashby S (2017) Classifying common wetland plants using hyperspectral data to identify optimal spectral bands for species mapping using a small unmanned aerial systems — A case study. IEEE International Geoscience and Remote Sensing Symposium (IGARSS) Fort Worth, TX, USA. 5924-5927. https://doi.org/10.1109/IGARSS.2017.8128357

Sharma RC (2022) Countrywide Mapping of Plant Ecological Communities with 101 Legends including Land Cover Types for the First Time at 10 m Resolution through Convolutional Learning of Satellite Images. Appl. Sci. 12(14):7125. https://doi.org/10.3390/app12147125

Statistics Canada (2017) Division No. 15, CDR [Census division], Alberta and Alberta [Province] (table).Government of Canada. https://www12.statcan.gc.ca/census-recensement/2016/dp-pd/prof/index.cfm?Lang=E . Accessed 27 August 2023

Stumpf A, Malet JP, Allemand P, Ulrich P (2014) Surface reconstruction and landslide displacement measurements with Pléiades satellite images. 95:1-12. https://doi.org/10.1016/j.isprsjprs.2014.05.008

Tang TY, Fu BL, Lou PQ, Bi L (2020) Segnet-Based Extraction of Wetland Vegetation Information from Uav Images. ISPRS Ann. Photogramm. Remote Sens. Spatial Inf. Sci. XLII-3/W10:375–380. https://doi.org/10.5194/isprs-archives-XLII-3-W10-375-2020

Teng J, Xia S, Liu Y, Yu X, Duan H, Xiao H, Zhao C (2021) Assessing habitat suitability for wintering geese by using Normalized Difference Water Index (NDWI) in a large floodplain wetland, China. Ecol. Indic. 122:107260. https://doi.org/10.1016/j.ecolind.2020.107260

Thiel C, Mueller MM, Epple L, Thau C, Hese S, Voltersen M, Henkel A (2020) UAS Imagery-Based Mapping of Coarse Wood Debris in a Natural Deciduous Forest in Central Germany (Hainich National Park). Remote Sens. 12(20):3293. https://doi.org/10.3390/rs12203293

Thompson DK, Simpson BN, Beaudoin A (2016) Using forest structure to predict the distribution of treed boreal peatlands in Canada. For. Ecol. Manage. 372:19-27. https://doi.org/10.1016/j.foreco.2016.03.056

Tian S, Zhang X, Tian J, Sun Q (2016) Random Forest Classification of Wetland Landcovers from Multi-Sensor Data in the Arid Region of Xinjiang, China. Remote Sens. 8(11):954. https://doi.org/10.3390/rs8110954

Tonia D, McKean JA, Benjankar RM, Wright CW, Goode JR, Chen Q, Reeder WJ, Carmichael RA, Edmondson MR (2018) Mapping river bathymetries: Evaluating topobathymetric LiDAR survey. Earth Surf. Processes Landforms 44(2):507-520. https://doi.org/10.1002/esp.4513

Torgersen CE, Faux RN, McIntosh BA, Poage NJ, Norton DJ (2001) Airborne thermal remote sensing for water temperature assessment in rivers and streams. Remote Sens. Environ. 76(3):386-398. https://doi.org/10.1016/S0034-4257(01)00186-9

Torresani M, Kleijn D, Reinier de Vries JP, Bartholomeus H, Chieffallo L, Gatti RC, Moudrý V, Da Re D, Tomelleri E, Rocchini D (2023) A novel approach for surveying flowers as a proxy for bee pollinators using drone images. Ecol. Indic. 149:110123. https://doi.org/10.1016/j.ecolind.2023.110123

Trimble (2022) eCognition Developer. Trimble Geospatial. https://docs.ecognition.com/v10.3.0 . Accessed 27 August 2023

United States Environmental Protection Agency (2022) What is a Wetland? United States Environmental Protection Agency. https://www.epa.gov/wetlands/what-wetland . Accessed 8 March 2022

Valencia E, Changoluisa I, Palma K, Cruz P, Valencia D, Ayala P, Hidalgo V, Quisi D, Jara N, Puga D (2022) Wetland monitoring technification for the Ecuadorian Andean region based on a multi-agent framework. Heliyon 8(3):e09054. https://doi.org/10.1016%2Fj.heliyon.2022.e09054

Van Hulse J, Koshgoftaar T (2009) Knowledge discovery from imbalanced and noisy data. Data Knowl. Eng. 68(12):1513-1542. https://doi.org/10.1016/j.datak.2009.08.005

Wang J, He T, Lin Y, (2018) Changes in ecological, agricultural, and urban land space in 1984-2012 in China: Land policies and regional social-economic drivers. Habitat International 71:1-13. https://doi.org/10.1016/j.habitatint.2017.10.010

Watson KB, Ricketts T, Galford G, Polasky S, O'Niel-Dunne J (2016) Quantifying flood mitigation services: The economic value of Otter Creek wetlands and floodplains to Middlebury, VT. Ecol. Econ. 130:16-24. https://doi.org/10.1016/j.ecolecon.2016.05.015

Weise K, Höfer R, Franke J, Guelmami A, Simonson W, Muro J, O'Connor B, Strauch A, Flink S, Eberle J, Mino E, Thulin S, Philipson, Van Valkengoed E, Truckenbrodt J, Zander F, Sánchez A, Schröder C, Thonfeld F, Fitoka E, Hilarides L (2020) Wetland extent tools for SDG 6.6.1 reporting from the Satellite-based Wetland Observation Service (SWOS). Remote Sens. Environ. 247:111892. https://doi.org/10.1016/j.rse.2020.111892

Wikum DA, Shanholtzer GF (1978) Application of the Braun-Blanquet cover-abundance scale for vegetation analysis in land development studies. Environ. Manage. 2:323-329. https://doi.org/10.1007/BF01866672

White L, McGovern M, Hayne S, Touzi R, Pasher J, Duffe J (2020) Investigating the Potential Use of RADARSAT-2 and UAS imagery for Monitoring the Restoration of Peatlands. Remote Sens. 12(15):2383. https://doi.org/10.3390/rs12152383

Wu Q, Lane CR (2016) Delineation and Quantification of Wetland Depressions in the Prairie Pothole Region of North Dakota. Wetlands 36:215-227. https://doi.org/10.1007/s13157-015-0731-6

Wu Q, Lane CR (2017) Delineating wetland catchments and modeling hydrologic connectivity using lidar data and aerial imagery. Hydrol. Earth Syst. Sci. 21:3579–3595. https://doi.org/10.5194/hess-21-3579-2017

Xing L, Niu Z (2019) Mapping and analyzing China's wetlands using MODIS time series data. Wetlands Ecol. Manage. 27:693-710. https://doi.org/10.1007/s11273-019-09687-y

Yu X, Guo X (2021) Extracting Fractional Vegetation Cover from Digital Photographs: A Comparison of In Situ, SamplePoint, and Image Classification Methods. Sensors 21(21):7310. https://doi.org/10.3390/s21217310

Zhang H, Feng Y, Guan W, Cao X, Li Z, Ding J (2021) Using unmanned aerial vehicles to quantify spatial patterns of dominant vegetation along an elevation gradient in the typical Gobi region in Xinjiang, Northwest China. Global Ecol. Conserv. 27:e01571. https://doi.org/10.1016/j.gecco.2021.e01571

Zhang W, Wang M-H, Hu J, Ho Y-S (2010) A review of published wetland research, 1991-2008: Ecological engineering and ecosystem restoration. Ecol. Eng. 36(8): 973-980. https://doi.org/10.1016/j.ecoleng.2010.04.029

Zheng Y, Niu Z, Gong P, Li M, Hu L, Wang L, Yang Y, Gu H, Mu J, Dou G, Xue H (2017) A method for alpine wetland delineation and features of border: Zoigê Plateau, China. Chin. Geogr. Sci. 27(5):784-799. http://doi.org/10.1007/s11769-017-0897-3

Zhou W, Wu N, Shi R, Wang Z (2022) UAV Mapping of the Chlorophyll Content in a Tidal Flat Wetland Using a Combination of Spectral and Frequency Indices. Remote Sens. 14(4):827. https://doi.org/10.3390/rs14040827

Zhu X, Hou Y, Weng Q, Chen L (2019) Integrating UAV optical imagery and LiDAR data for assessing the spatial relationship between mangrove and inundation across a subtropical

estuarine wetland. ISPRS J. Photogramm. Remote Sens. 149:146-156. https://doi.org/10.1016/j.isprsjprs.2019.01.021

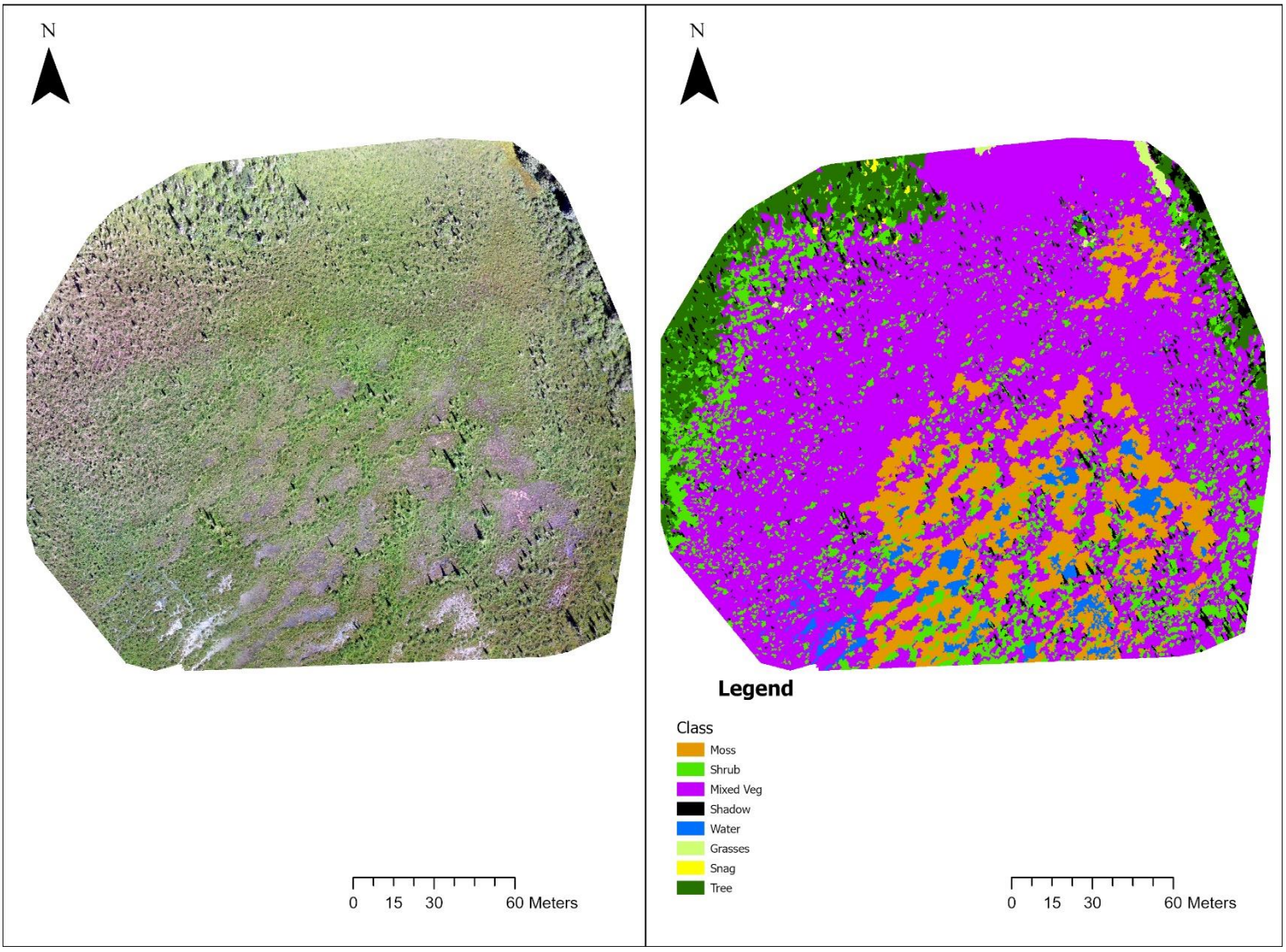
Zhu X, Meng L, Zhang Y, Weng Q, Morris J (2019) Tidal and meteorological influences on the growth of invasive Spartina alterniflora: evidence from UAV remote sensing. Remote Sens. 11(10):1208. https://doi.org/10.3390/rs11101208

Zweig CL, Burgess MA, Percival FH, Kitchens WM (2015) Use of Unmanned Aircraft Systems to Delineate Fine-Scale Wetland Vegetation Communities. Wetlands 35:303-309. https://doi.org/10.1007/s13157-014-0612-4

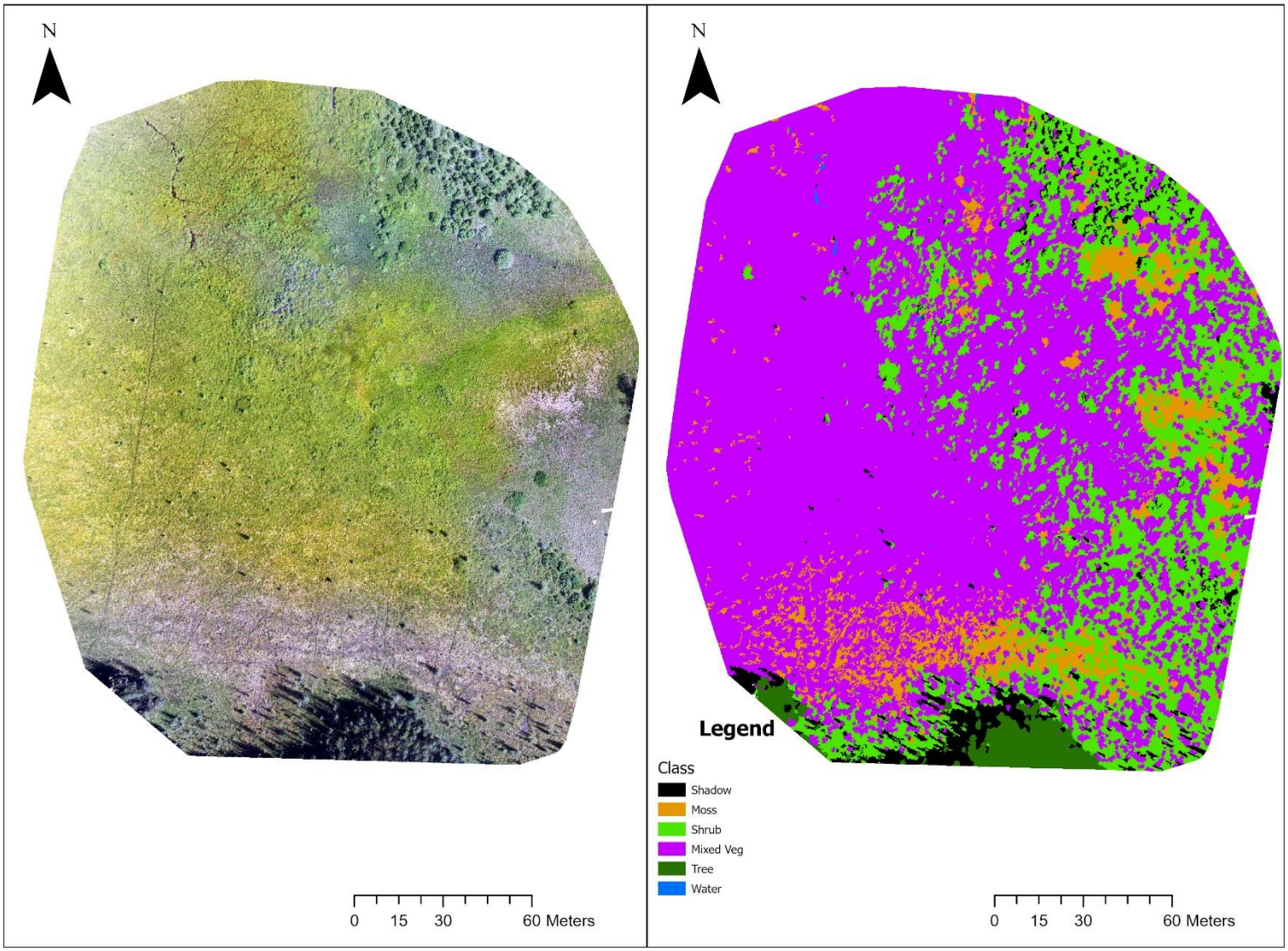
Appendix A

Maps (Increasing in Elevation)

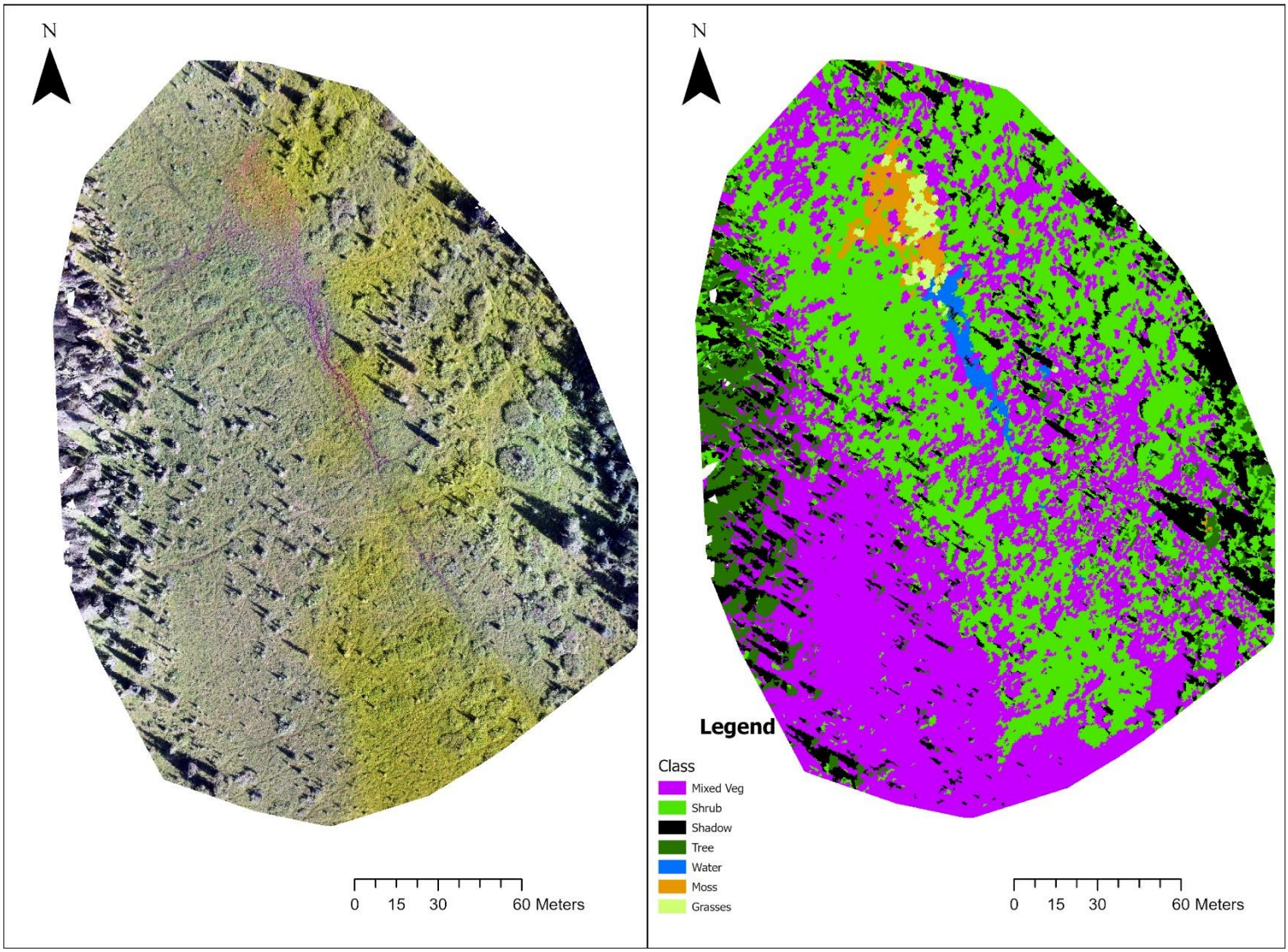
Site No. 7 (Subregion: Montane | Elevation: 1419m)



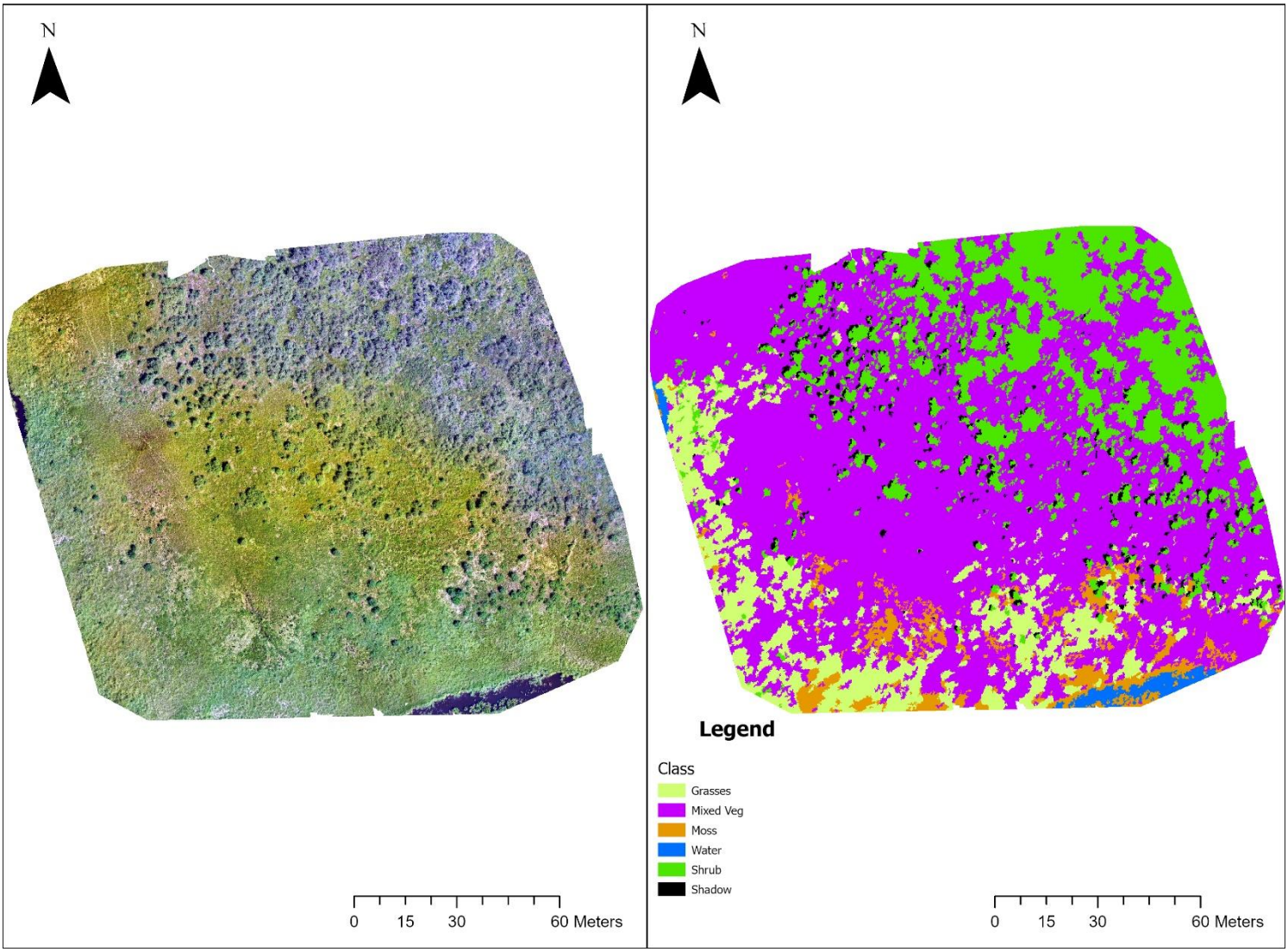
Site No. 12 (Subregion: Montane | Elevation: 1465m)



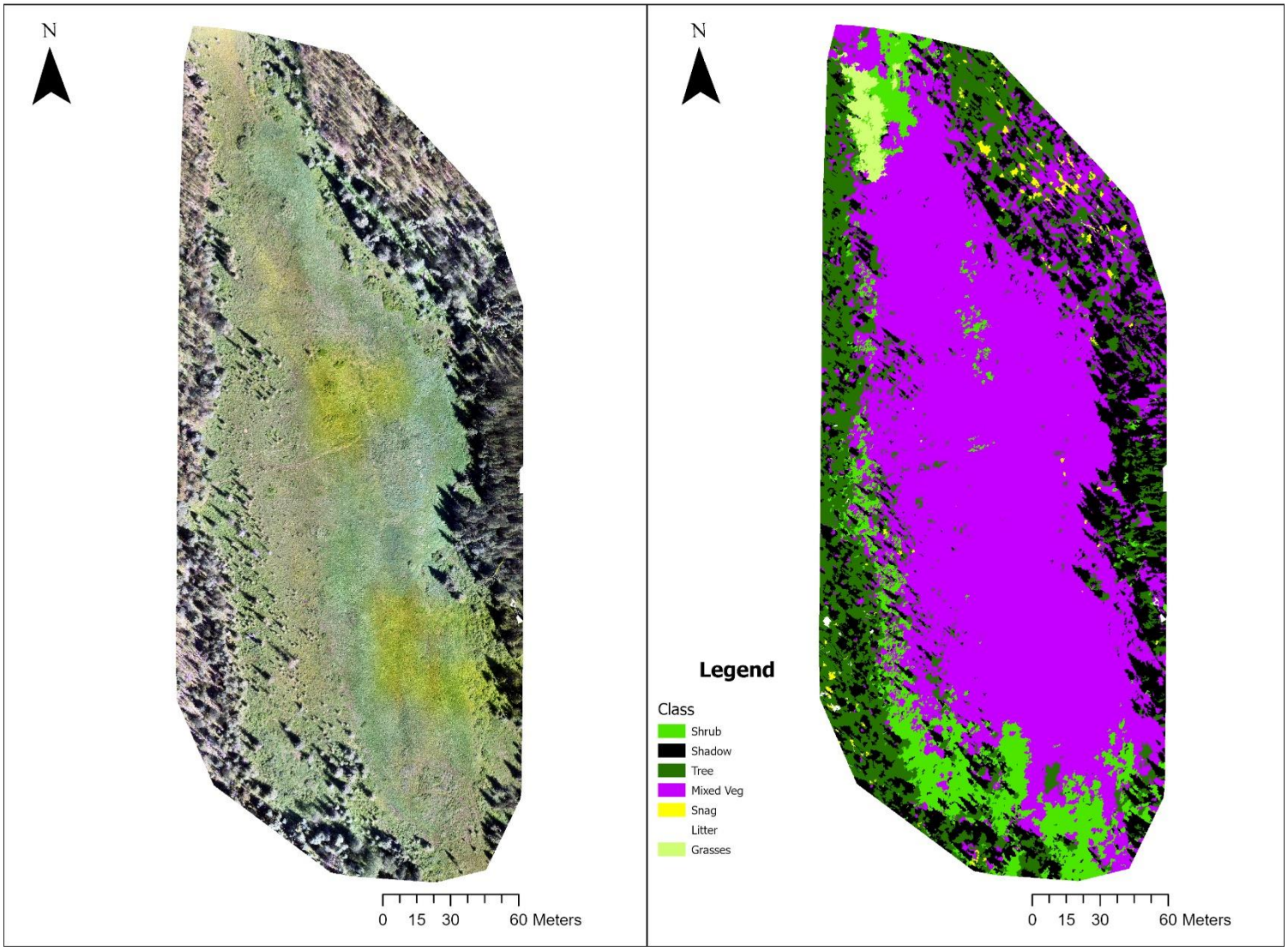
Site No. 9 (Subregion: Montane | Elevation: 1478m)



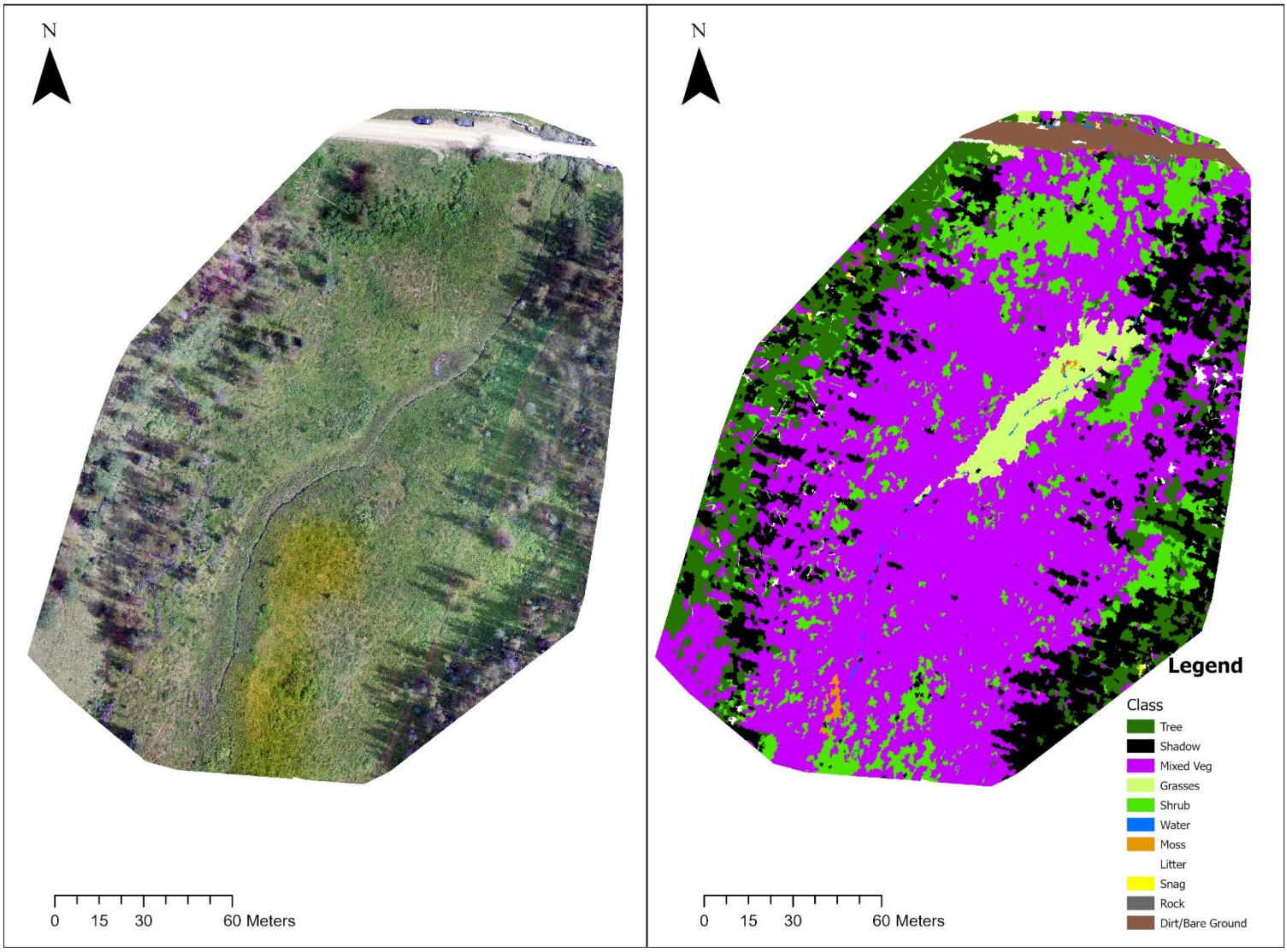
Site No. 16 (Subregion: Montane | Elevation: 1489m)



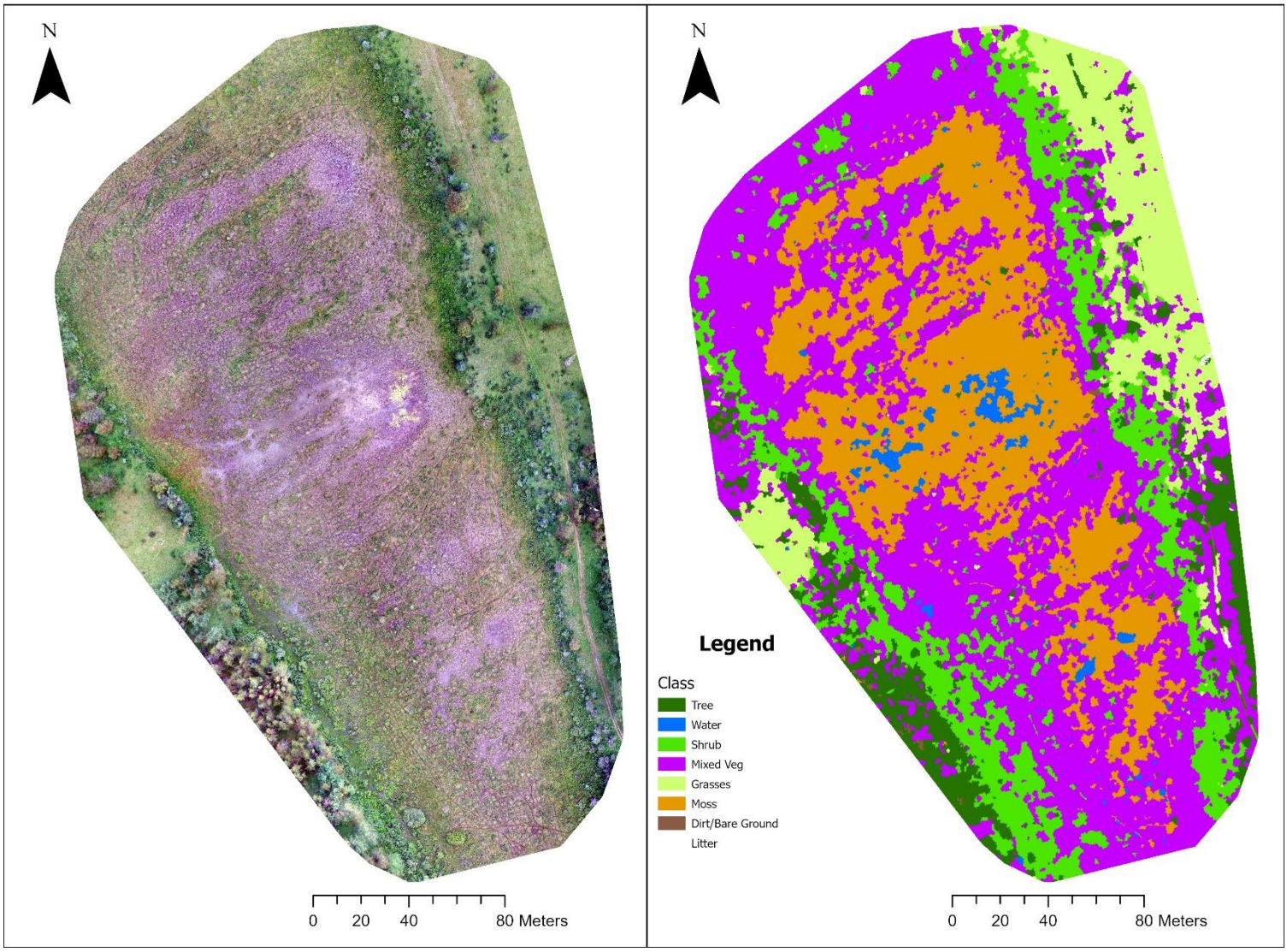
Site No. 10 (Subregion: Montane | Elevation: 1504m)



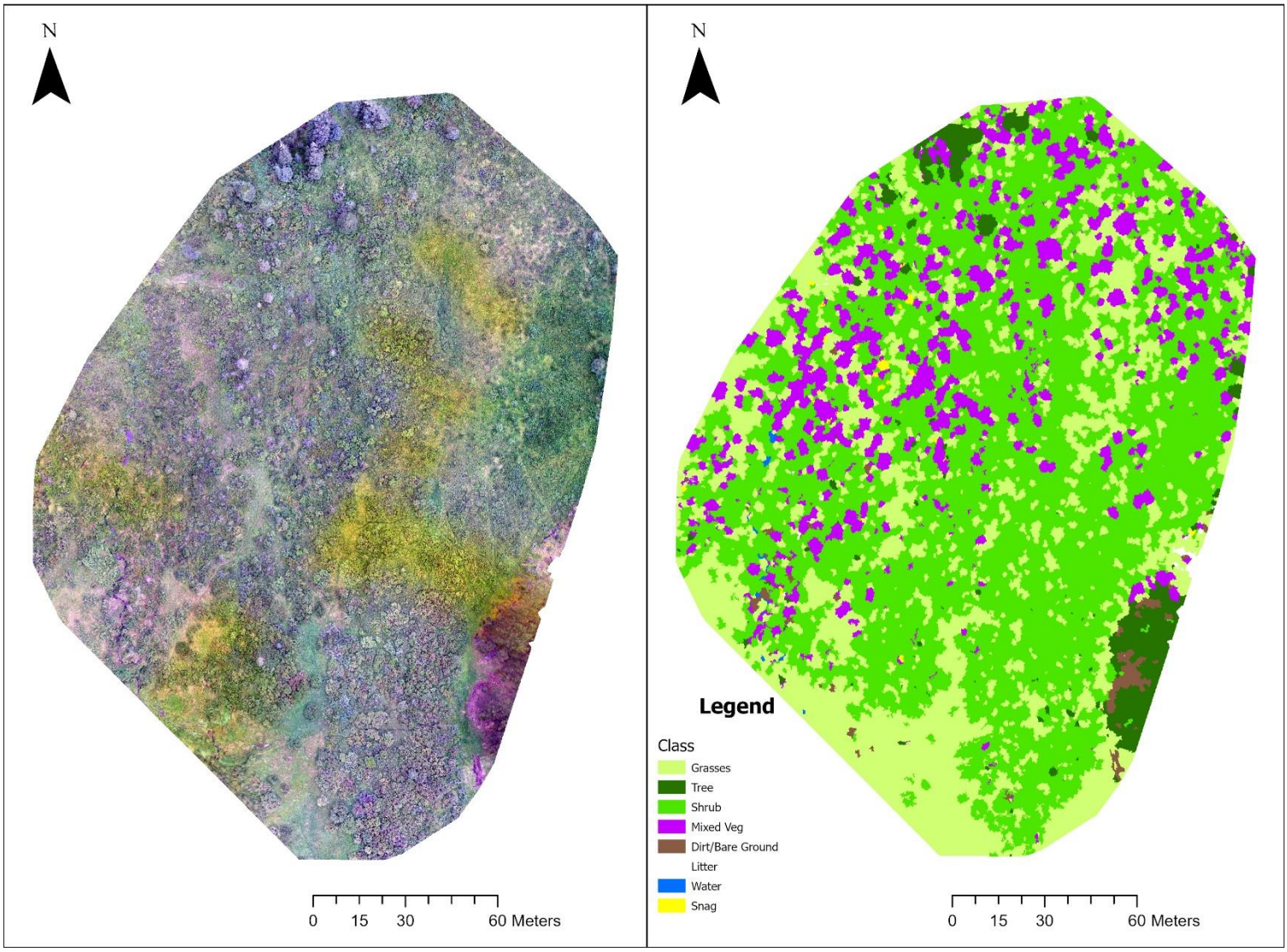
Site No. 17 (Subregion: Montane | Elevation: 1522m)



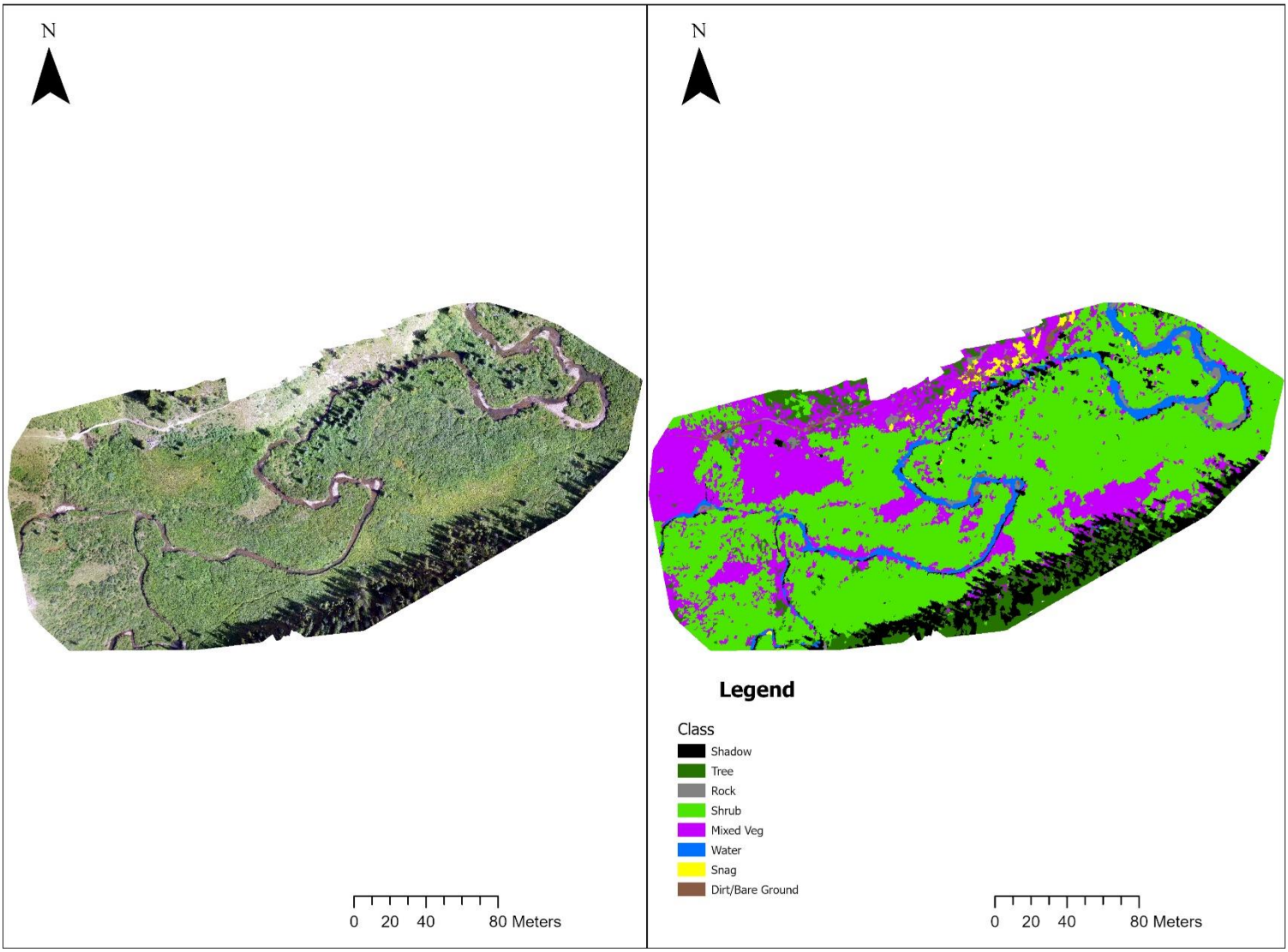
Site No. 4 (Subregion: Montane | Elevation: 1559m)



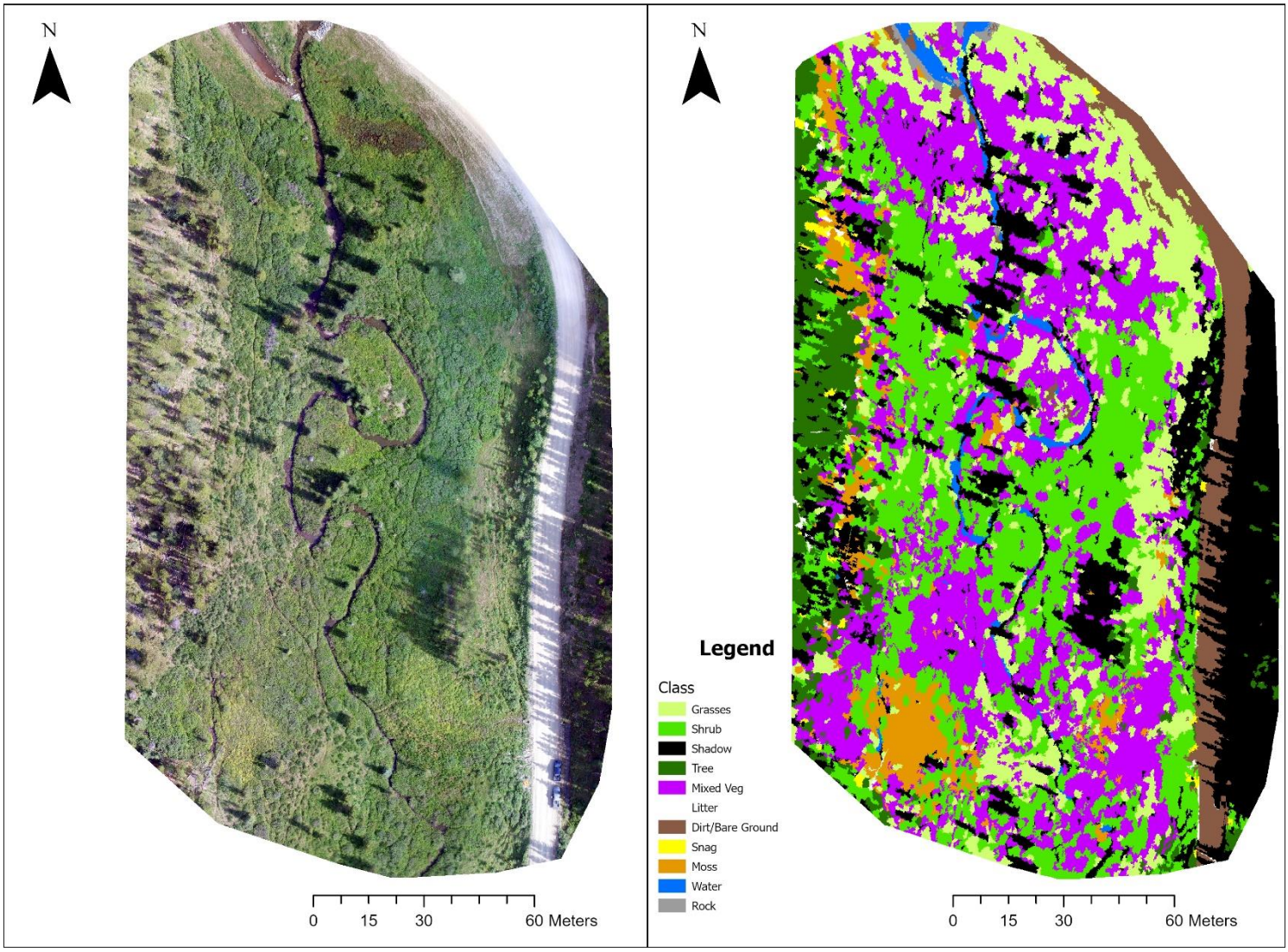
Site No. 1 (Subregion: Upper Foothills | Elevation: 1572m)



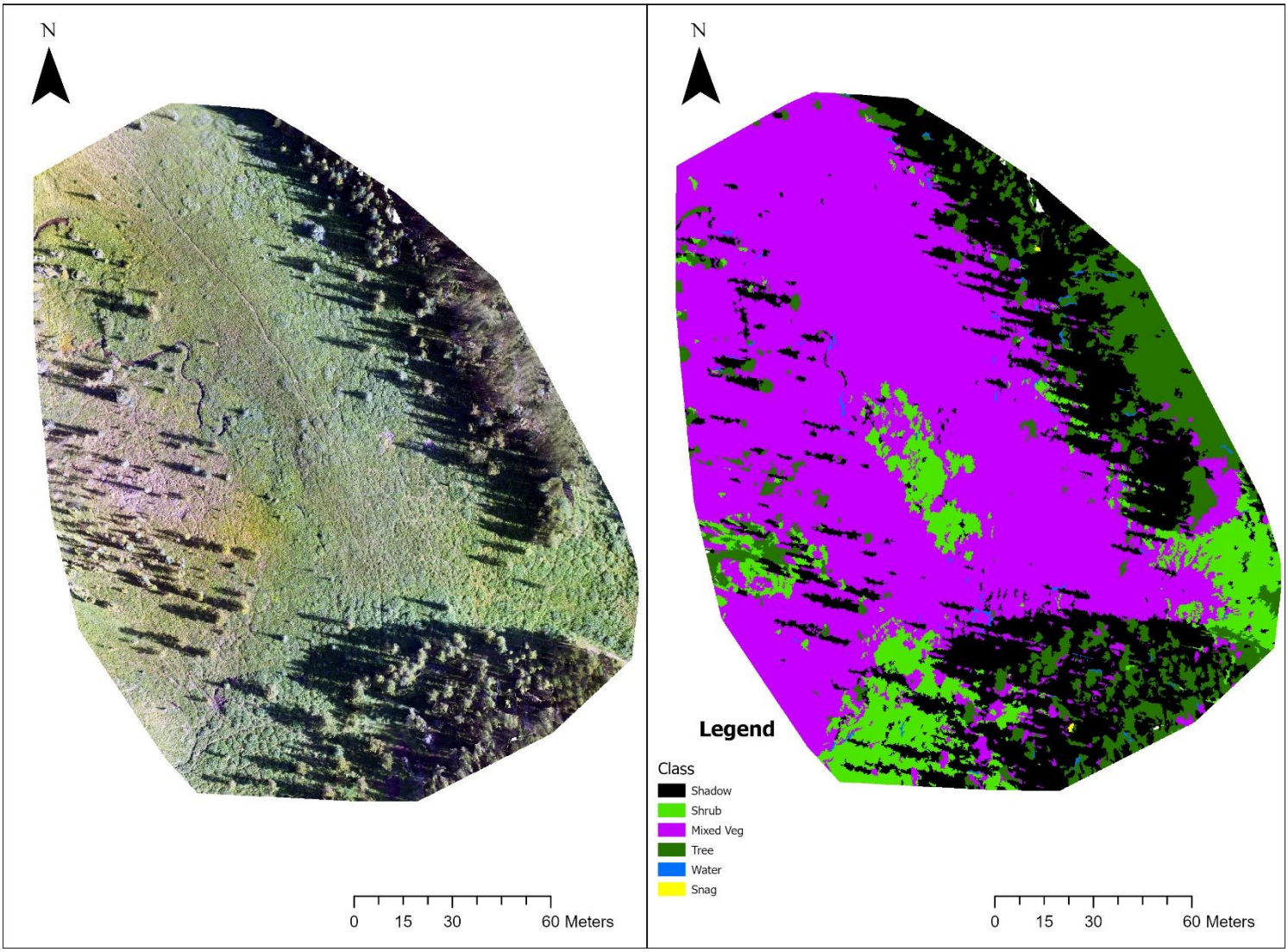
Site No. 13 (Subregion: Subalpine | Elevation: 1697m)



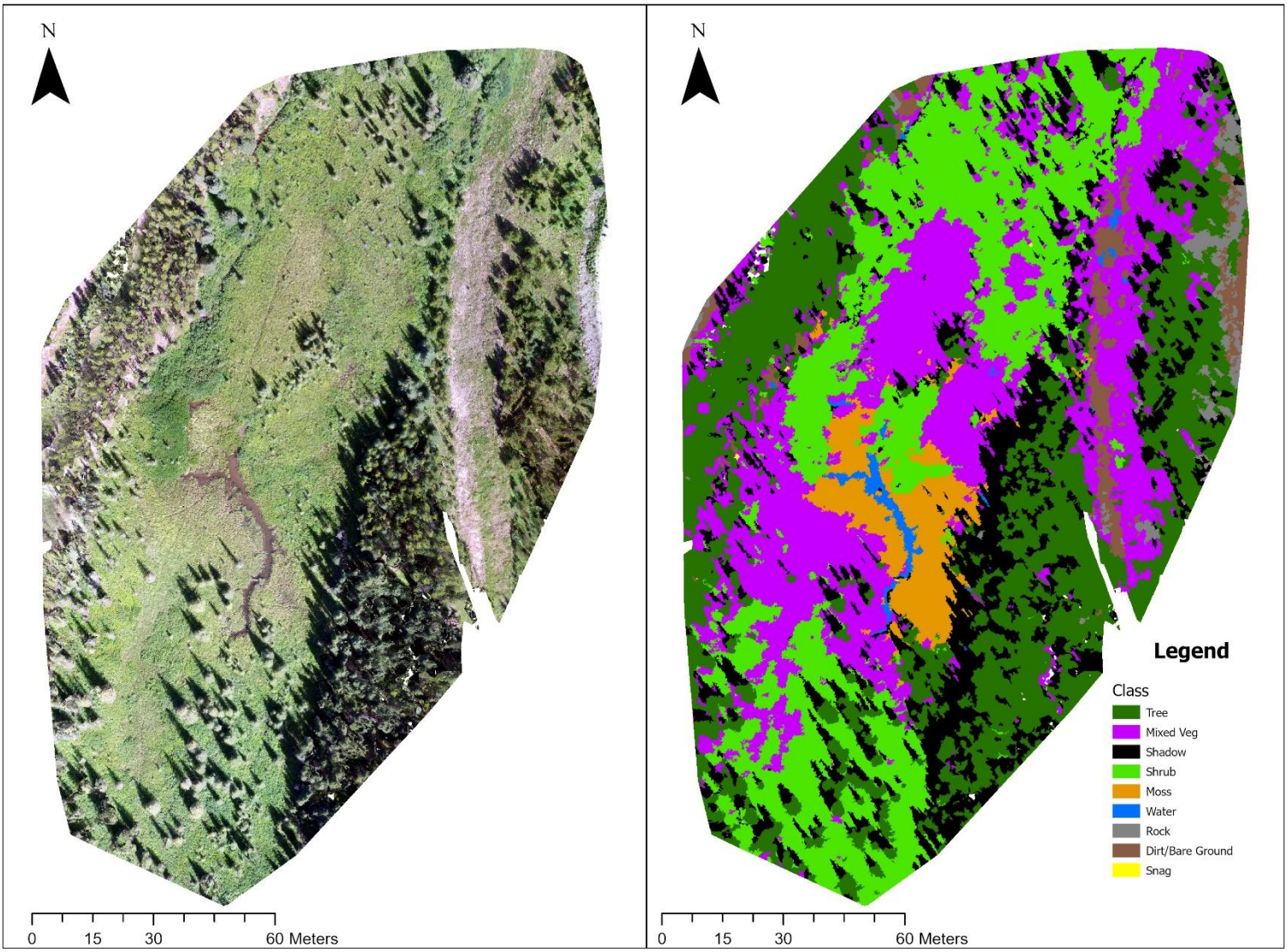
Site No. 2 (Subregion: Subalpine | Elevation: 1718m)



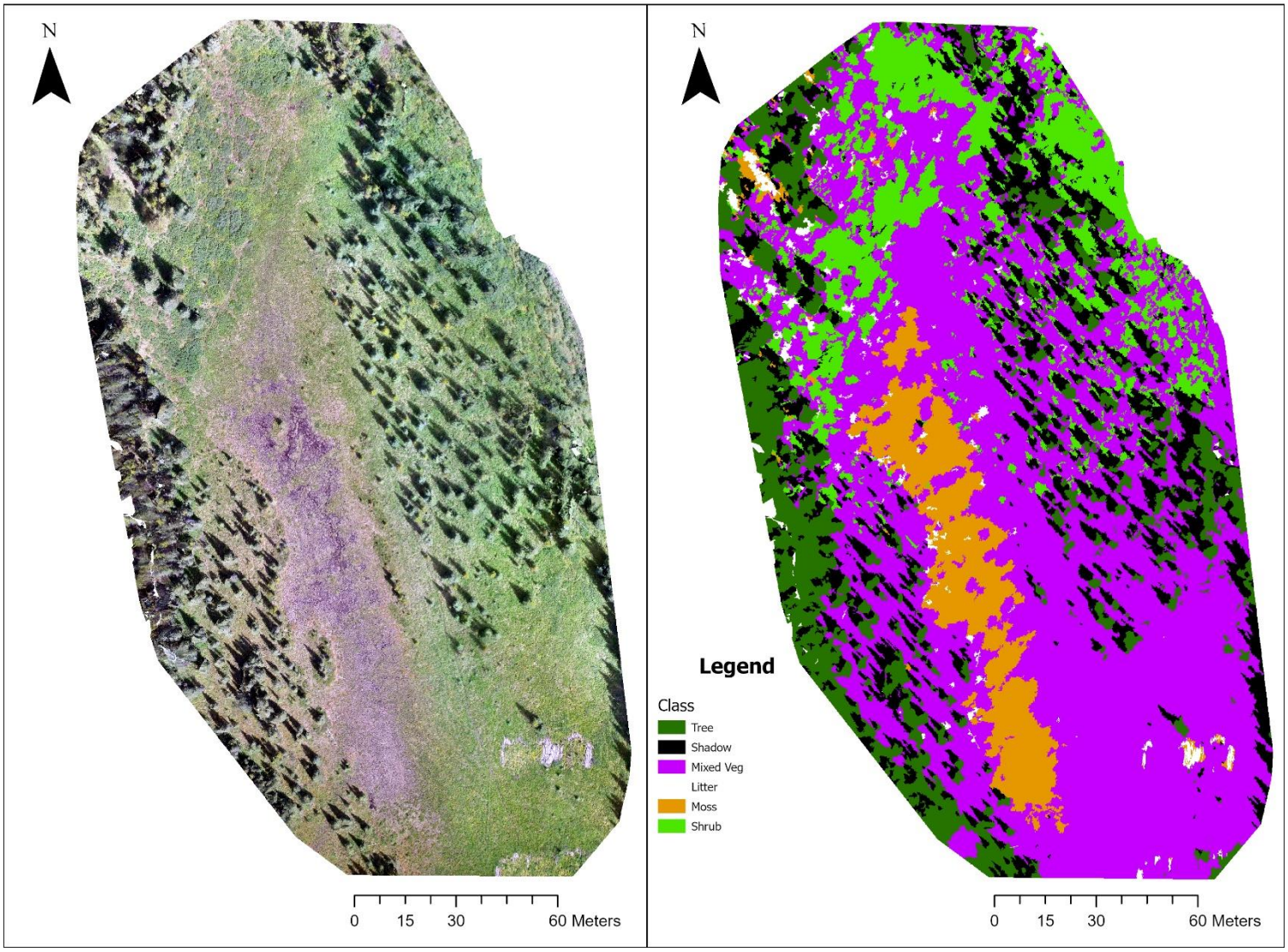
Site No. 15 (Subregion: Subalpine | Elevation: 1739m)



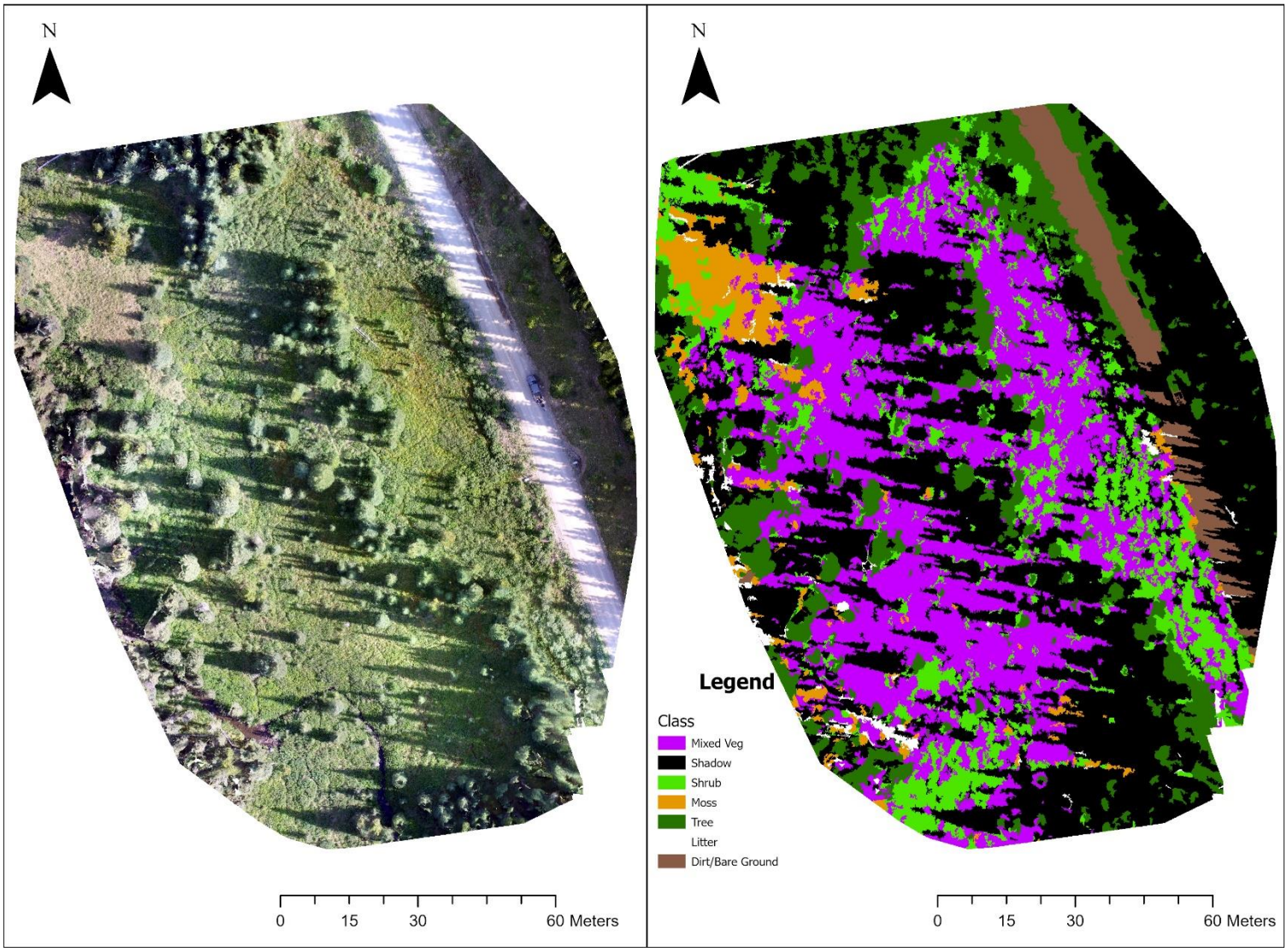
Site No. 11 (Subregion: Subalpine | Elevation: 1744m)



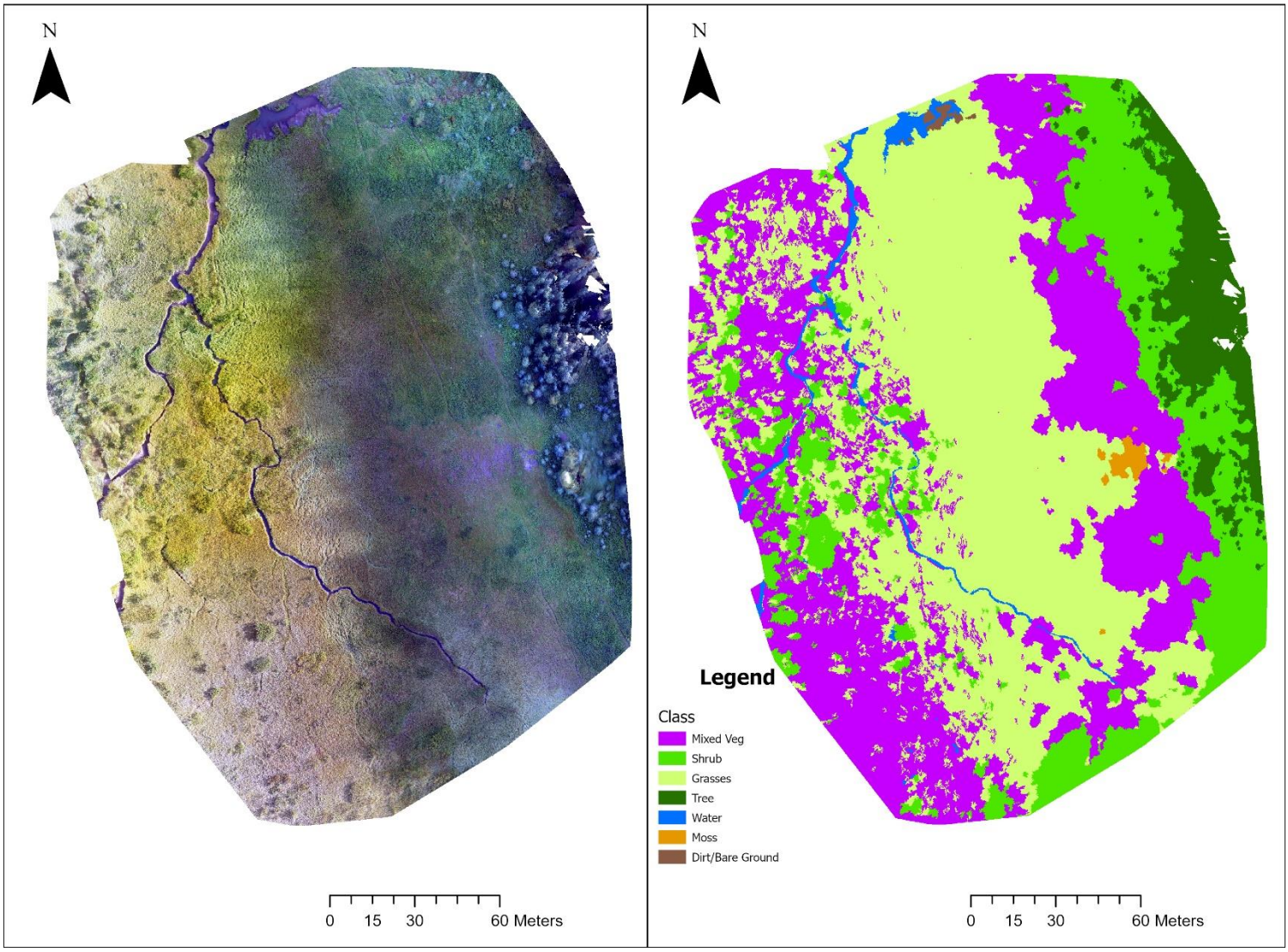
Site No. 14 (Subregion: Subalpine | Elevation: 1795m)



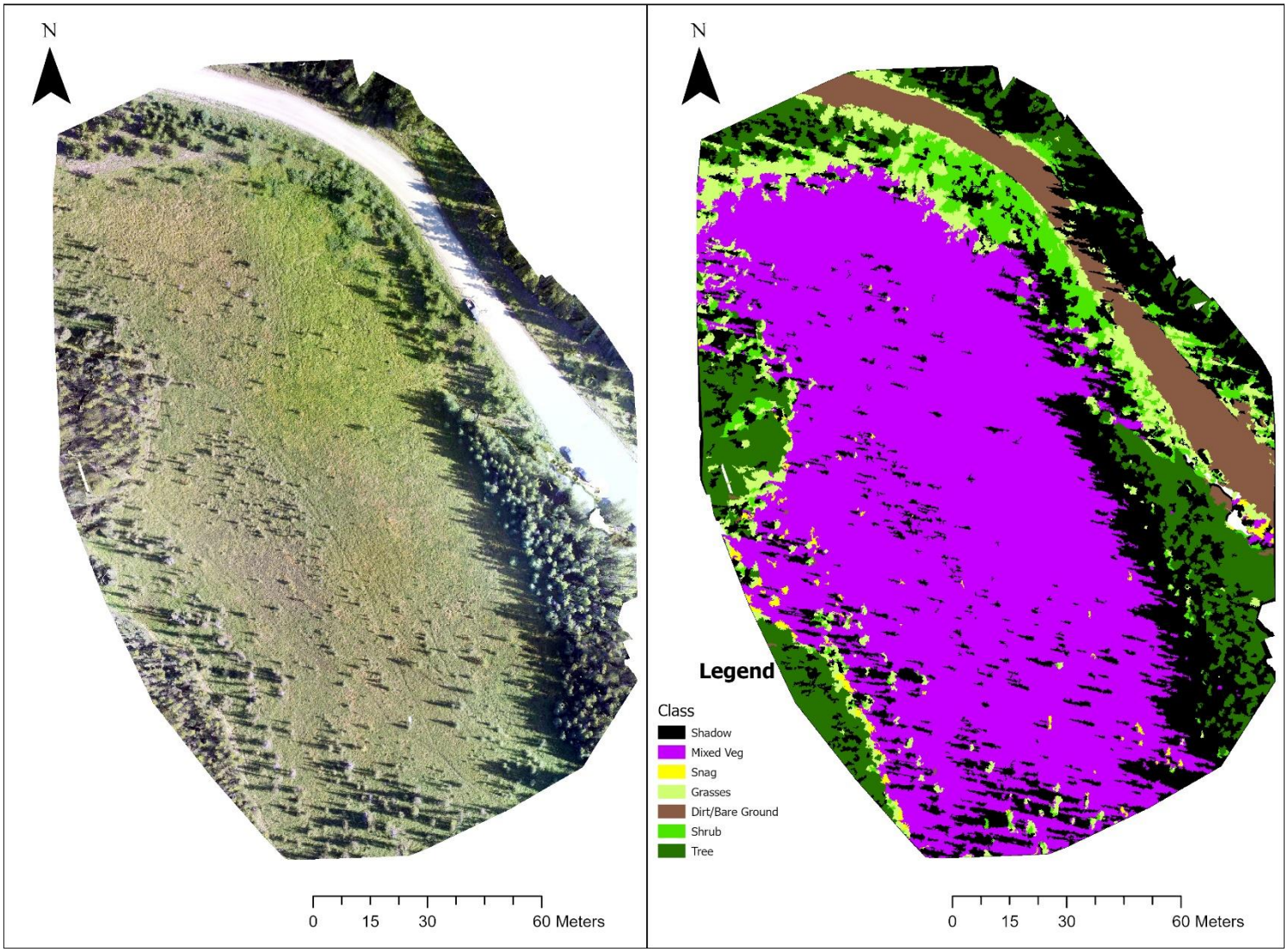
Site No. 18 (Subregion: Subalpine | Elevation: 1800m)



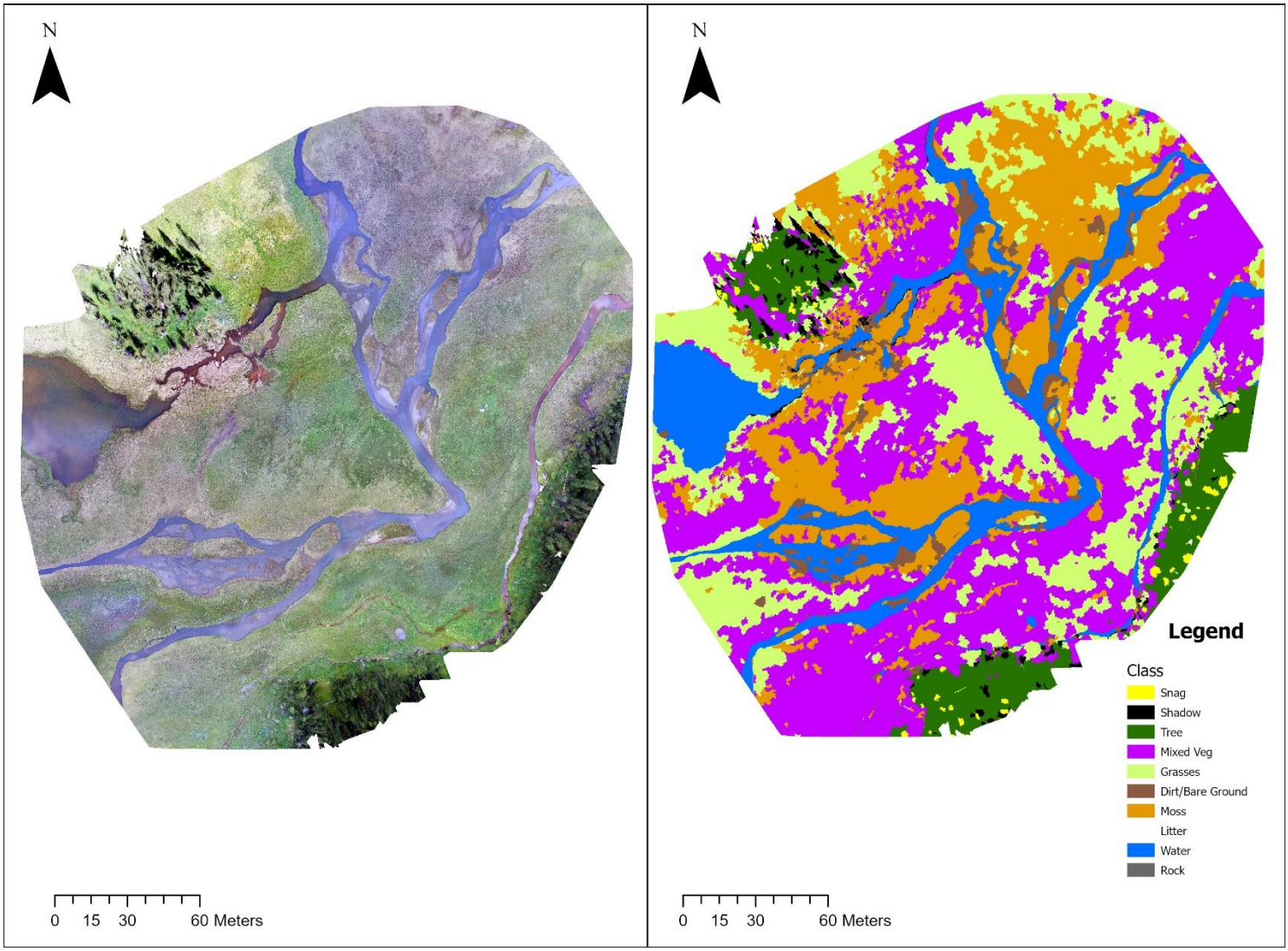
Site No. 5 (Subregion: Subalpine | Elevation: 1839m)



Site No. 3 (Subregion: Subalpine | Elevation: 1844m)



Site No. 6 (Subregion: Subalpine | Elevation: 1962m)



Site No. 8 (Subregion: Subalpine | Elevation: 2106m)

